Thermalization, evolution and observables in integrated hydrokinetic model of A+A collisions

Yu. Sinyukov, BITP, Kiev

EMMI Seminar

EMMI/GSI, Darmstadt, April 26, 2016

Integrated HydroKinetic model: HKM → iHKM

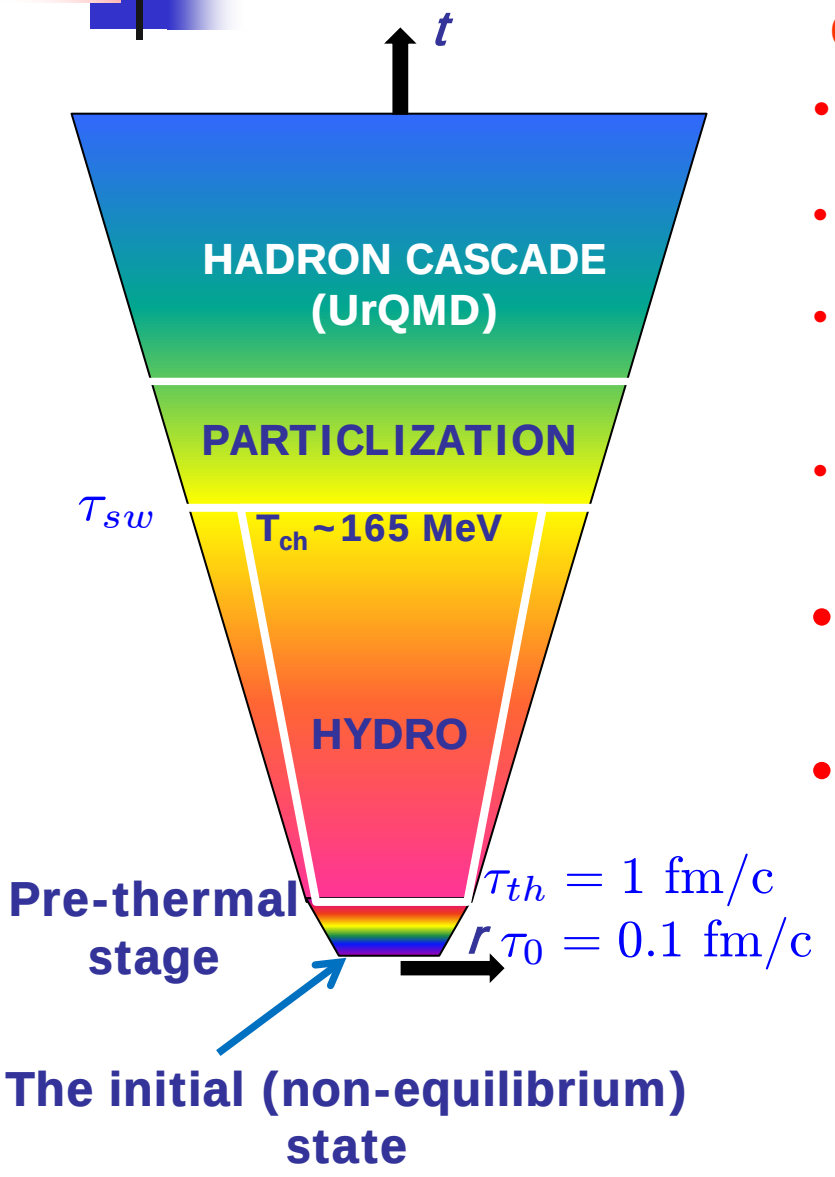

Complete algorithm incorporates the stages:

- **generation of the initial states**;
- **thermalization of initially non-thermal matter**;
- **viscous chemically equilibrated hydrodynamic expansion**;
- **sudden (with option: continuous) particlization of expanding medium**;
- **a switch to UrQMD cascade with near equilibrium hadron gas as input;**
- **simulation of observables.**

Yu.S., Akkelin, Hama: PRL 89 (2002) 052301;
... + Karpenko: PRC 78 (2008) 034906;
Karpenko, Yu.S. : PRC 81 (2010) 054903;
... PLB 688 (2010) 50;
Akkelin, Yu.S. : PRC 81 (2010) 064901;
Karpenko, Yu.S., Werner: PRC 87 (2013) 024914;
Naboka, Akkelin, Karpenko, Yu.S. : PRC **91** (2015) 014906;
Naboka, Karpenko, Yu.S. Phys. Rev. C **93** (2016) 024902.

.

Initial states

The most commonly used models of initial state are:

High Energies

MC-G (Monte Carlo Glauber)
MC-KLN (Monte Carlo Kharzeev-Levin-Nardi)
EPOS (parton-based Gribov-Regge model)
EKRT (perturbative QCD + saturation model)
IP-Glasma (Impact Parameter dependent Glasma)

Low Energies

MC-G (Monte Carlo Glauber) - ?
UrQMD (Ultra-Relativistic Molecular Dynamics) - ?

PROBLEM:

No one model leads to the proper matter thermalization, while the biggest experimental discovery for a few decades is that hydrodynamics is the basis of the "Standard Model " of high energy A+A collisions

MC-G Initial State (IS) attributed to $\tau_0 = 0.1$ fm/c

GLISSANDO 2

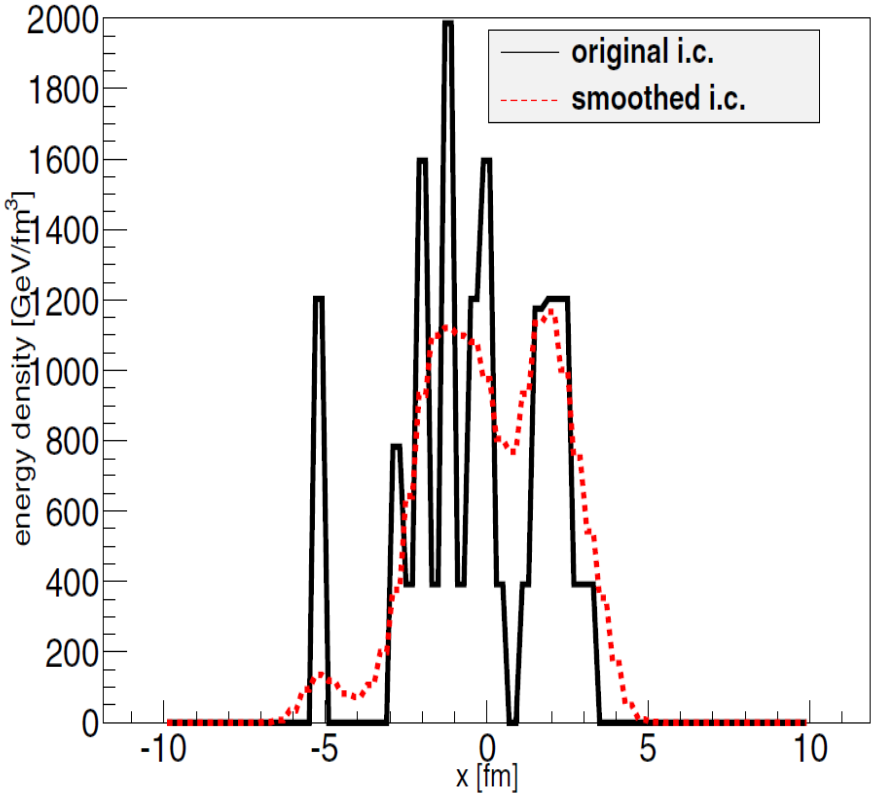

- The initial state (IS) is highly inhomogenious.
- It is not locally equilibrated.
- The IS most probable is strongly momentum anisotropic (result from CGC)

$$f(t_{\sigma_0}, \mathbf{r}_{\sigma_0}, \mathbf{p}) = \epsilon(b; \tau_0, \mathbf{r}_T) f_0(p)$$

$$T^{\mu\nu}_{\text{free}}(x) = \int d^3p \frac{p^\mu p^\nu}{p_0} f_{\sigma_0}(x,p); T^{00}[f_0(p)] = 1$$

$$f_0^*(p) \propto \exp\left(-\sqrt{\frac{p_T^2}{\lambda_\perp^2} + \frac{p_L^2}{\lambda_\parallel^2}}\right)$$

Florkowski et al

MC-G Hybrid for ensemble of ISs

$$\epsilon(b; \tau_0, \mathbf{r}_T) = \epsilon_0 \frac{(1-\alpha) N_W(b, \mathbf{r}_T)/2 + \alpha N_{bin}(b, \mathbf{r}_T)}{(1-\alpha) N_W(b=0, \mathbf{r}_T=0)/2 + \alpha N_{bin}(b=0, \mathbf{r}_T=0)}$$

Parameters of IS

$$\Lambda = \lambda_\perp / \lambda_\parallel$$

ϵ_0, α = 0.24 [4]

Multiplicity dependence of all charged particles on centrality

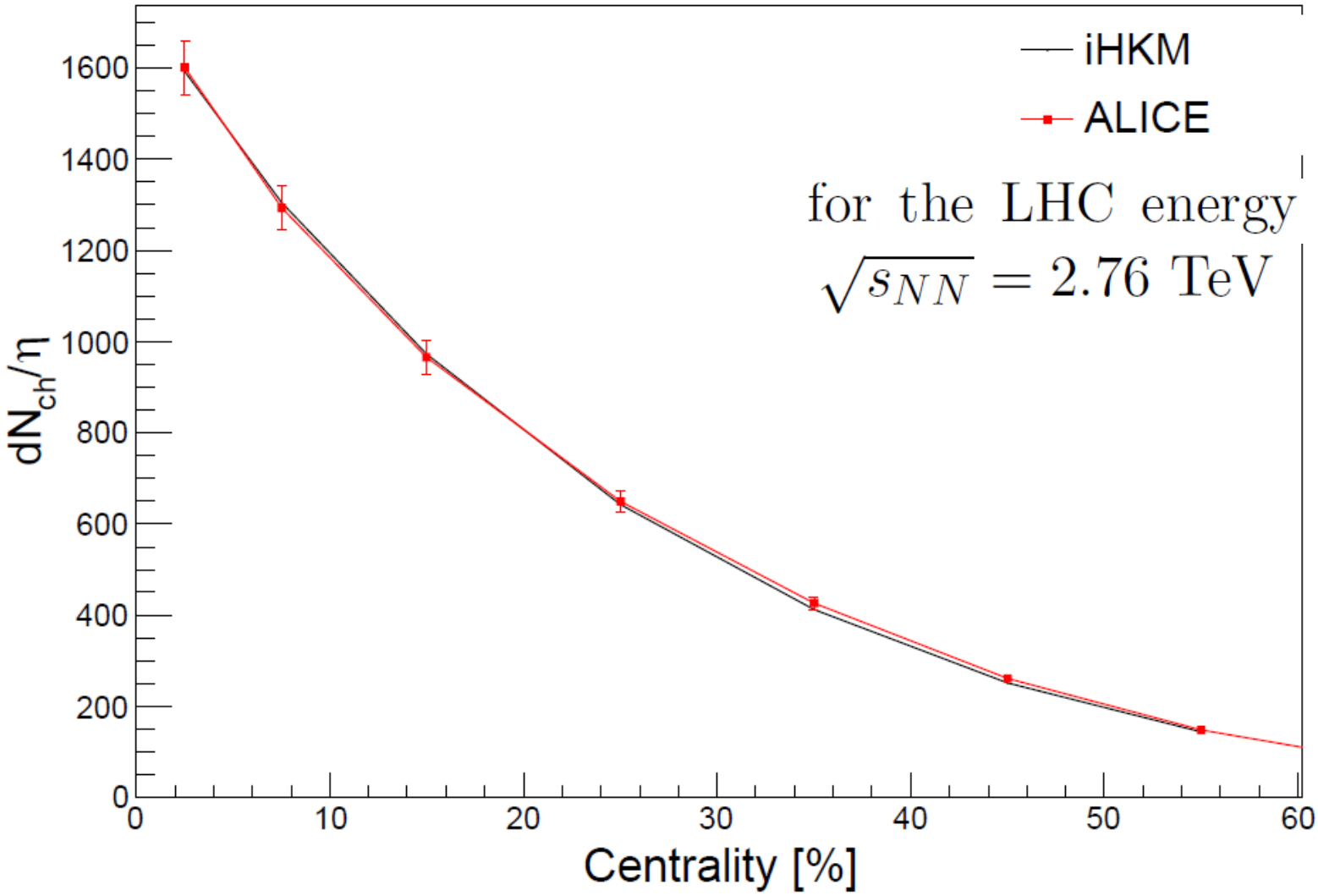

parameter values : $\tau_0 = 0.1$ fm/c, $\tau_{rel} = 0.25$ fm/c, $\eta/s = 0.08$, $\Lambda = 100$

Pre-thermal stage (thermalization)

Akkelin, Yu.S. :PRC **81** (2010); Naboka, Akkelin, Karpenko, Yu.S. : PRC **91** (2015).

Non-thermal state $\tau_0 = 0.1$ fm/c $\longrightarrow$ locally near equilibrated state $\tau_{th} = 1$ fm/c

Boltzmann equation in relaxation time approximation (integral form) **MAIN OBJECT**

$$\mathcal{P}_\sigma(x,p) = \exp\Big(-\int_t^{t_\sigma} \frac{d\bar{t}}{\tau_{rel}(\overline{x},p)}\Big)$$

$$\overline{x} \equiv (\bar{t}, \mathbf{x}_\sigma + (\mathbf{p}/p_0)(\bar{t} - t_\sigma))$$

MAIN ANSATZ with minimal number of parameters: $\tau_0,\ \tau_{th},\ \tau_{rel}$

$$\mathcal{P}_{\tau_0\to\tau}(\tau) = \left(\frac{\tau_{th}-\tau}{t_{th}-\tau_0}\right)^{\frac{\tau_{th}-\tau_0}{\tau_{\rm rel}(\tau_0)}} \Longrightarrow T^{\mu\nu}(x) = T^{\mu\nu}_{\rm free}(x)\mathcal{P}(\tau) + T^{\mu\nu}_{\rm hyd}(x)(1-\mathcal{P}(\tau))$$

$$\Longrightarrow 0 \le \mathcal{P}(\tau) \le 1,\ \mathcal{P}(\tau_0) = 1,\ \mathcal{P}(\tau_{th}) = 0,\ \partial_\mu \mathcal{P}(\tau)_{\tau_{\rm th}} = 0$$

MAIN EQUATIONS

$$\partial_{;\mu}\widetilde{T}^{\mu\nu}_{\rm hyd}(x) = -T^{\mu\nu}_{\rm free}(x)\partial_{;\mu}\mathcal{P}(\tau)$$

where $\begin{cases} \tilde{T}^{\mu\nu}_{\rm hyd} = [1-\mathcal{P}(\tau)]T^{\mu\nu}_{\rm hyd} \\ \widetilde{\pi}^{\mu\nu} = \pi^{\mu\nu}(1-\mathcal{P}) \end{cases}$

$$(1-\mathcal{P}(\tau))\left\langle u^\gamma \partial_{;\gamma}\frac{\widetilde{\pi}^{\mu\nu}}{(1-\mathcal{P}(\tau))}\right\rangle = -\frac{\widetilde{\pi}^{\mu\nu} - (1-\mathcal{P}(\tau))\pi^{\mu\nu}_{\rm NS}}{\tau_\pi} - \frac{4}{3}\widetilde{\pi}^{\mu\nu}\partial_{;\gamma}u^\gamma$$

$\Lambda = 1$ $\tau_{rel} = 0.5$ fm/c $\lambda = 100$

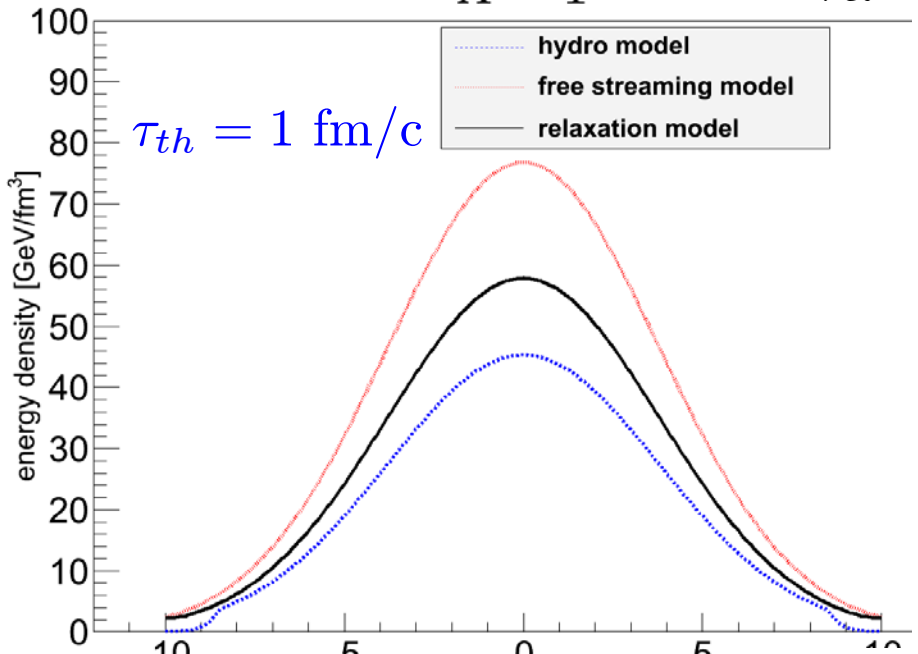

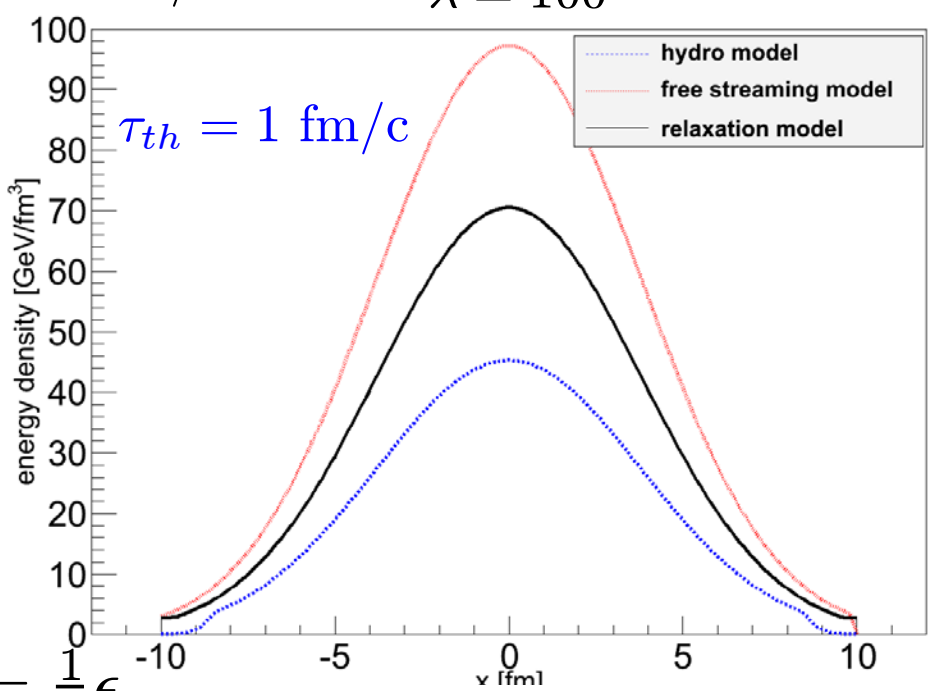

$p = \frac{1}{3}\epsilon$

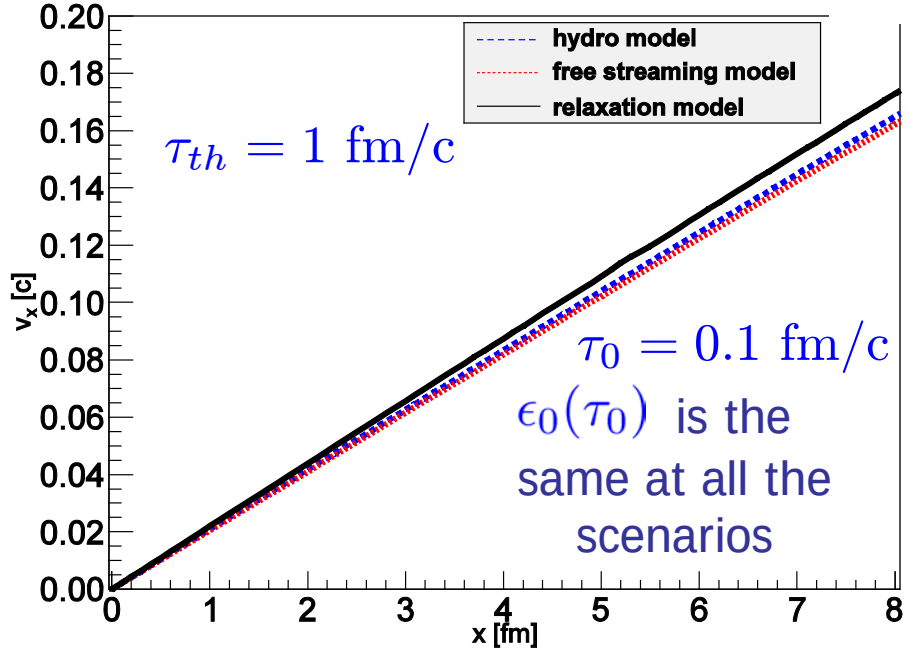

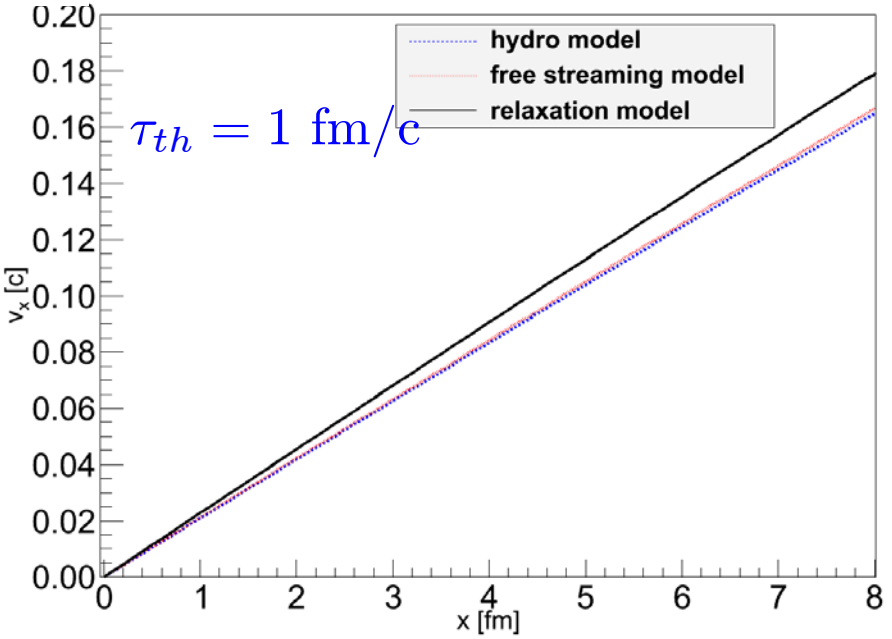

The other stages: Hydro evolution, particlization, hadronic cascade

- **Hydro evolution:** $\tau \leq \tau_{th}$ $\tau \geq \tau_{th}$

$$T^{\mu\nu}(x) = T^{\mu\nu}_{\rm free}(x)\mathcal{P}(\tau) + T^{\mu\nu}_{\rm hyd}(x)(1-\mathcal{P}(\tau)) \rightarrow T^{\mu\nu}_{\rm hyd}(x)$$
$$= (\epsilon_{\rm hyd}(x) + p_{\rm hyd}(x) + \Pi)u^{\mu}_{\rm hyd}(x)u^{\nu}_{\rm hyd}(x)$$
$$-(p_{\rm hyd}(x) + \Pi)g^{\mu\nu} + \pi^{\mu\nu}.$$

IC is the result of pre-thermal evolutuon reached at τ_{th}

Solving of Israel-Stewart Relativistic Viscous Fluid Dynamics with Π =0

The other stages: Hydro evolution, particlization, hadronic cascade

- **Hydro evolution:** $\tau \leq \tau_{th}$ $\tau \geq \tau_{th}$

$$T^{\mu\nu}(x) = T^{\mu\nu}_{\rm free}(x)\mathcal{P}(\tau) + T^{\mu\nu}_{\rm hyd}(x)(1-\mathcal{P}(\tau)) \rightarrow T^{\mu\nu}_{\rm hyd}(x)$$
$$= (\epsilon_{\rm hyd}(x) + p_{\rm hyd}(x) + \Pi)u^{\mu}_{\rm hyd}(x)u^{\nu}_{\rm hyd}(x)$$
$$-(p_{\rm hyd}(x) + \Pi)g^{\mu\nu} + \pi^{\mu\nu}.$$

Solving of Israel-Stewart Relativistic Viscous Fluid Dynamics with Π =0

- **Particlization:** at the isotherm hypersurface T=165 MeV

$$\text{energy density } \epsilon = 0.5 \text{ GeV/fm}^3 \text{ for the Laine-Schroeder EoS}$$

Switching hypersurface build with help of Cornelius routine.

For particle distribution the Grad's 14 momentum ansatz is used:

$$\frac{d^3\Delta N_i}{dp^* d(cos\theta) d\phi} = \frac{\Delta\sigma^*_\mu p^{*\mu}}{p^{*0}} p^{*2} f_{eq}\left(p^{*0}; T, \mu_i\right)\left[1 + (1 \mp f_{eq})\frac{p^*_\mu p^*_\nu \pi^{*\mu\nu}}{2T^2(\epsilon + p)}\right]$$

The other stages: Hydro evolution, particlization, hadronic cascade

- **Hydro evolution:** $\tau \leq \tau_{th}$ $T^{\mu\nu}(x) = T^{\mu\nu}_{\rm free}(x)\mathcal{P}(\tau) + T^{\mu\nu}_{\rm hyd}(x)(1-\mathcal{P}(\tau)) \rightarrow T^{\mu\nu}_{\rm hyd}(x)$ $\tau \geq \tau_{th}$

$$= (\epsilon_{\rm hyd}(x) + p_{\rm hyd}(x) + \Pi)u^{\mu}_{\rm hyd}(x)u^{\nu}_{\rm hyd}(x) - (p_{\rm hyd}(x) + \Pi)g^{\mu\nu} + \pi^{\mu\nu}.$$

Solving of Israel-Stewart Relativistic Viscous Fluid Dynamics with Π =0

- **Particlization:** at the isotherm hypersurface T=165 MeV

$$\text{energy density } \epsilon = 0.5 \text{ GeV/fm}^3 \text{ for the Laine-Schroeder EoS}$$

Switching hypersurface build with help of Cornelius routine.

For particle distribution the Grad's 14 momentum ansatz is used:

$$\frac{d^3\Delta N_i}{dp^* d(cos\theta) d\phi} = \frac{\Delta\sigma^*_\mu p^{*\mu}}{p^{*0}} p^{*2} f_{eq}\left(p^{*0}; T, \mu_i\right)\left[1 + (1 \mp f_{eq})\frac{p^*_\mu p^*_\nu \pi^{*\mu\nu}}{2T^2(\epsilon + p)}\right]$$

- **Hadronic cascade:** The above distribution function with Poisson distributions for each sort of particle numbers is the input for UrQMD cascade.

The other stages: Hydro evolution, particlization, hadronic cascade

- **Hydro evolution:** $\tau \leq \tau_{th}$

$$T^{\mu\nu}(x) = T^{\mu\nu}_{\rm free}(x)\mathcal{P}(\tau) + T^{\mu\nu}_{\rm hyd}(x)(1-\mathcal{P}(\tau)) = T^{\mu\nu}_{\rm hyd}(x)$$
$$= (\epsilon_{\rm hyd}(x) + p_{\rm hyd}(x) + \Pi)u^{\mu}_{\rm hyd}(x)u^{\nu}_{\rm hyd}(x)$$
$$-(p_{\rm hyd}(x) + \Pi)g^{\mu\nu} + \pi^{\mu\nu}.$$

Solving of Israel-Stewart Relativistic Viscous Fluid Dynamics with Π =0

- **Particlization:** at the isotherm hypersurface T=165 MeV

$$\text{energy density } \epsilon = 0.5 \text{ GeV/fm}^3 \text{ for the Laine-Schroeder EoS}$$

Switching hypersurface build with help of Cornelius routine.

For particle distribution the Grad's 14 momentum ansatz is used:

$$\frac{d^3\Delta N_i}{dp^* d(cos\theta) d\phi} = \frac{\Delta\sigma^*_\mu p^{*\mu}}{p^{*0}} p^{*2} f_{eq}\left(p^{*0}; T, \mu_i\right)\left[1 + (1 \mp f_{eq})\frac{p^*_\mu p^*_\nu \pi^{*\mu\nu}}{2T^2(\epsilon + p)}\right]$$

- **Hadronic cascade:** The above distribution function with Poisson distributions for each sort of particle numbers is the input for UrQMD

Details are in: Naboka, Karpenko, Yu.S. C **93** (2016) 024902

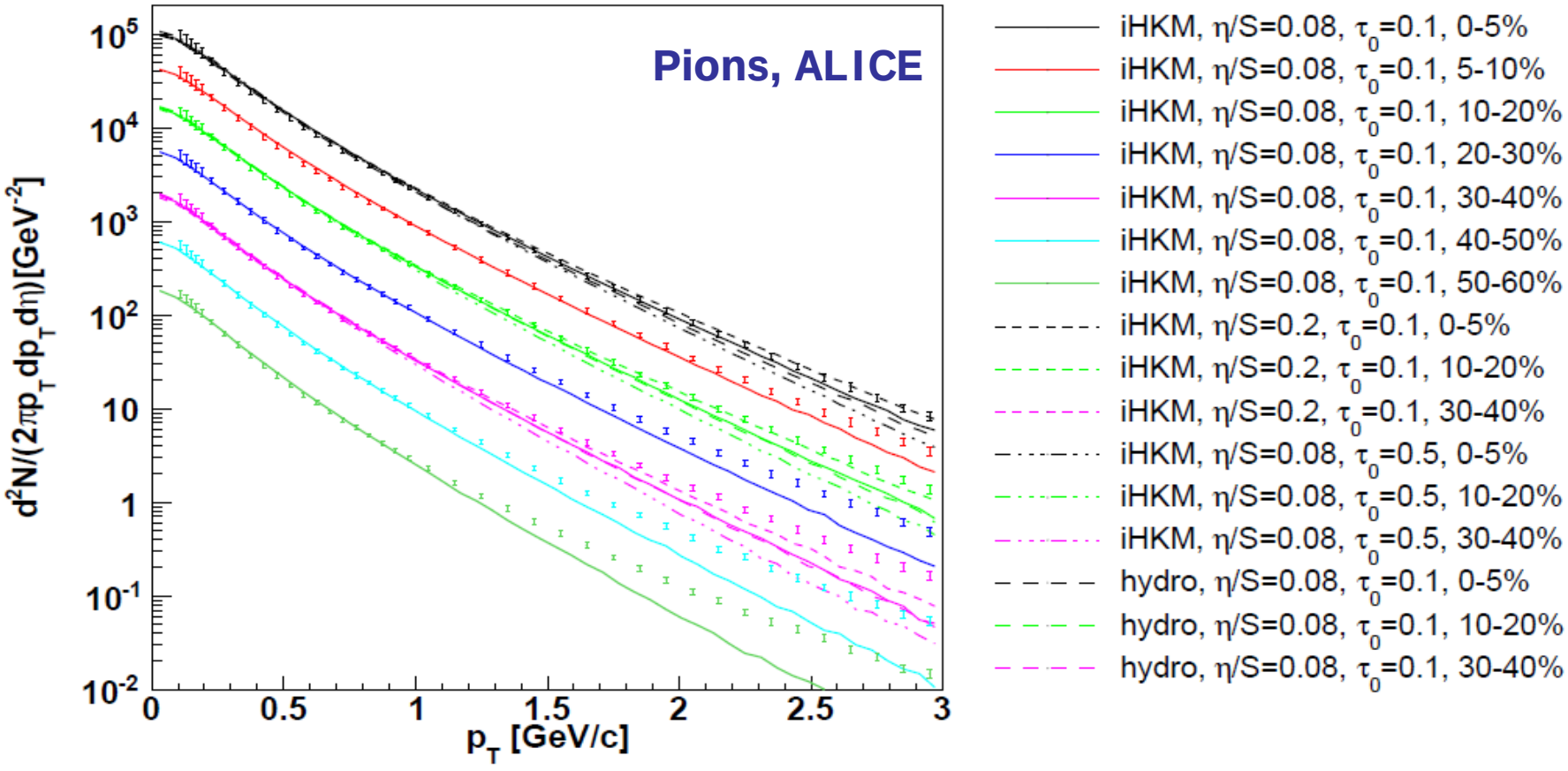

FIG. 2. Resulting pion spectra in the $0.1 < p_T < 3$ GeV/c region for centrality classes 0-5%, 5-10%, 10-20%, 20-30%, 30-40%, 40-50% and 50-60% obtained in the iHKM basic scenario (as in Fig. 1). The results are compared with those in iHKM at the other parameter $\tau_0 = 0.5$ fm/c and with pure viscous hydro at the starting time $\tau_{th} \to \tau_0 = 0.1$ fm/c for centrality classes 0-5%, 10-20%, 30-40%. The experimental data are from [31]. The spectra for different centralities are multiplied by the factor of 2 ($2^6 = 64$ for 0-5% centrality).

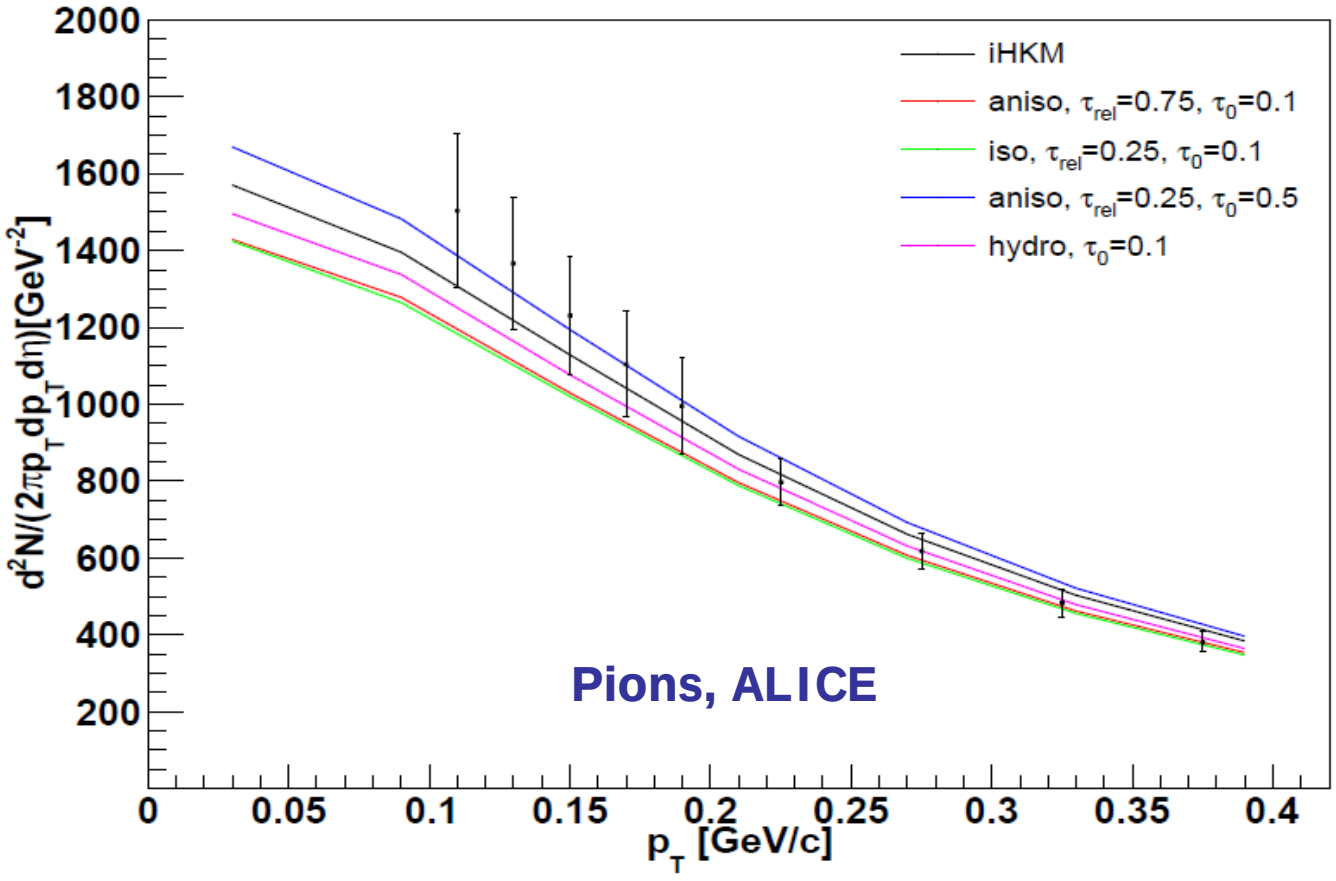

LHC,
Pion spectra
"under
microscope"
(linear scale)

FIG. 5. The detail picture of pion spectra in soft p_T region for 0-5% centrality in the iHKM basic scenario (as in Fig. 1) in comparison with the results obtained with (1) the other relaxation time $\tau_{rel} = 0.75$ fm/c instead of 0.25 fm/c, or with (2) isotropic parameter $\Lambda = 1$ instead of anisotropy one $\Lambda = 100$, or with (3) the other initial time $\tau_0 = 0.5$ fm/c instead of 0.1 fm/c. Also the results for pure viscous hydro, starting at $\tau_{th} \to \tau_0 = 0.1$ fm/c are presented. The experimental data are from [31].

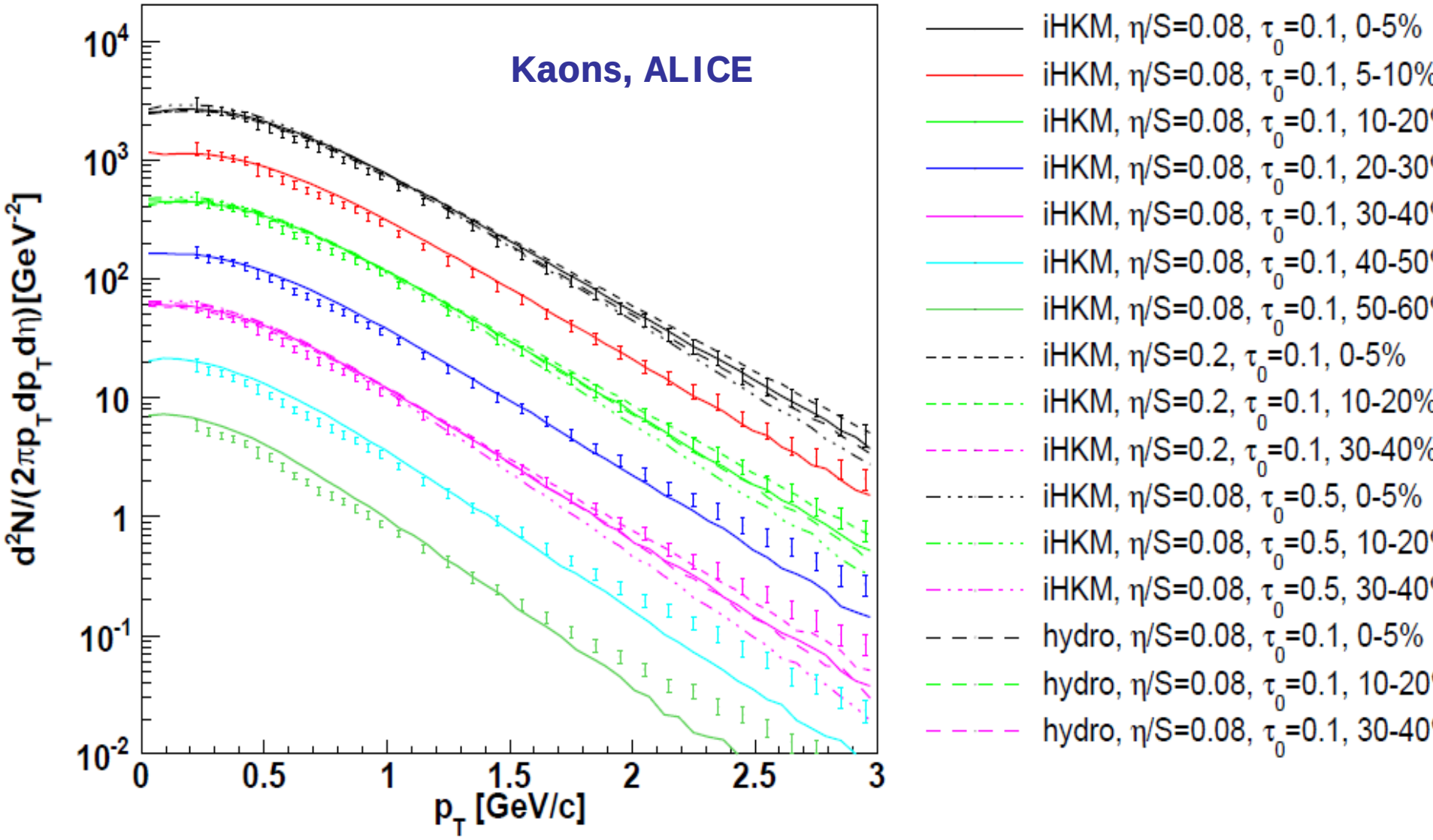

FIG. 3. The resulting kaon spectra under the same conditions as in Fig. 2.

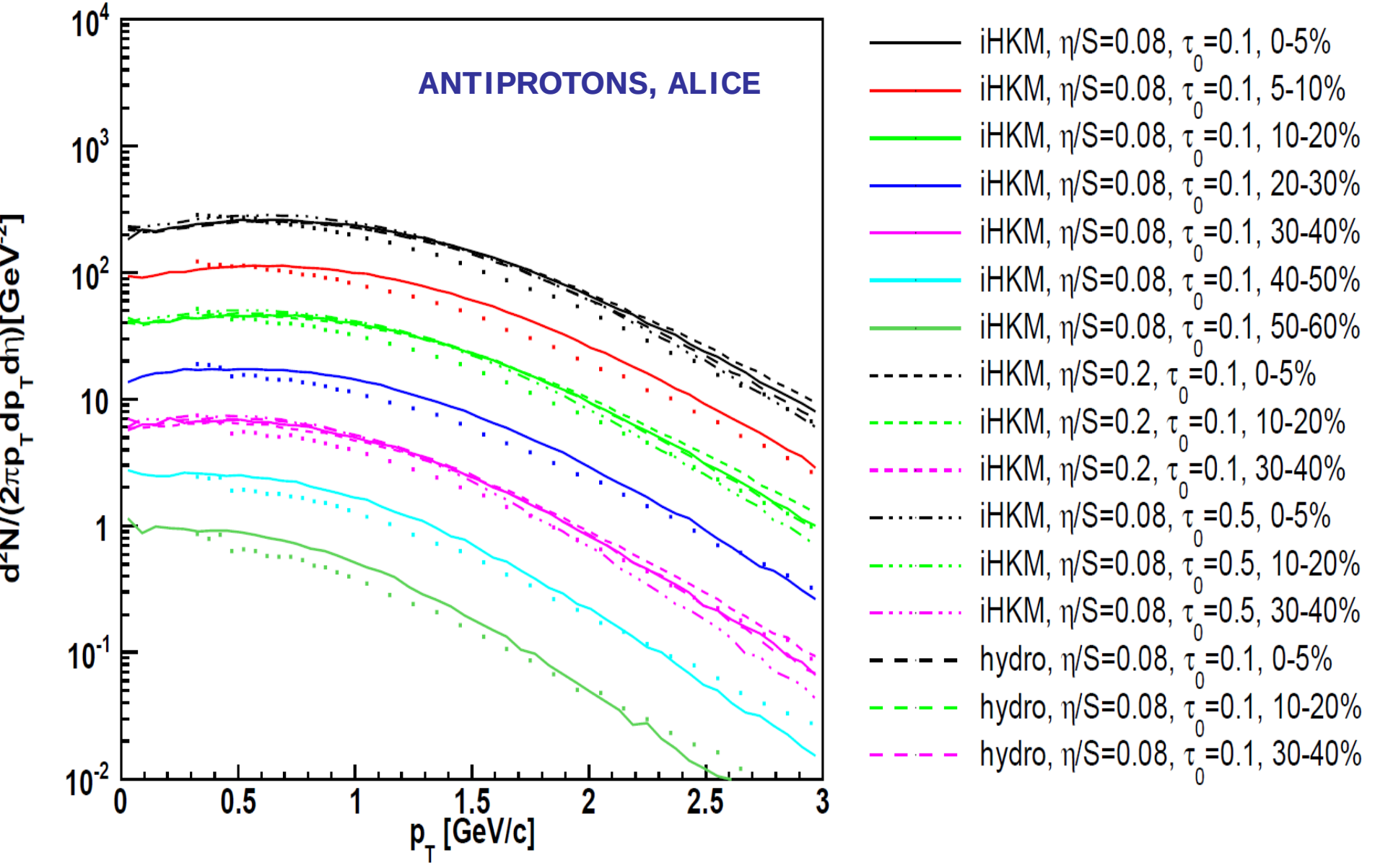

FIG. 4. The resulting antiproton spectra under the same conditions as in Fig. 2.

Predictions for particle spectra at LHC in non-central collisions

Centrality Dependence of π, K, p in Pb–Pb at $\sqrt{s_{NN}} = 2.76$ TeV

ALICE Collaboration

arXiv:1303.0737v1 [hep-ex]

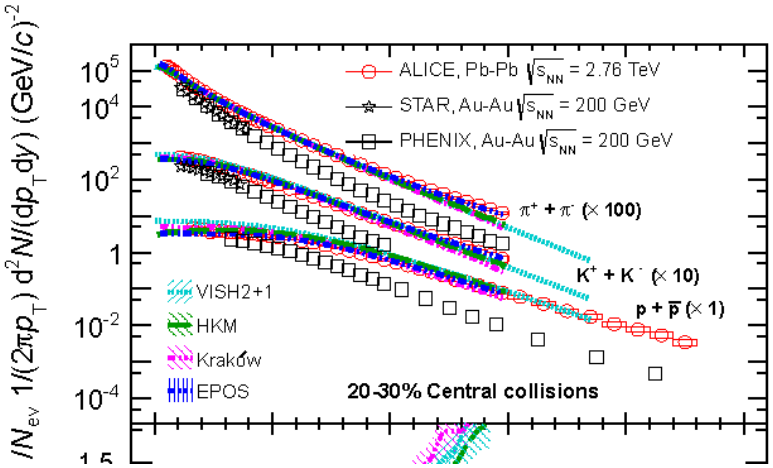

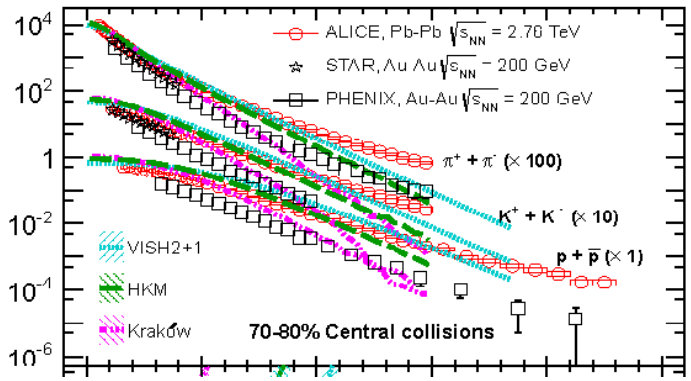

Quotations:

The difference between VISH2+1 and the data are possibly due to the lack of an explicit description of the hadronic phase in the model. This idea is supported by the comparison with HKM [47, 50]. HKM is a model similar to VISH2+1, in which after the hydrodynamic phase particles are injected into a hadronic cascade model (UrQMD), which further transports them until final decoupling. The hadronic phase builds up additional radial flow and affects particle ratios due to the hadronic interactions. As can be seen, this model yields a better description of the data. The protons at low p_T, and hence their total number, are rather well reproduced, even if the slope is significantly smaller than in the data. Antibaryon-baryon annihilation is an important ingredient for the description of particle yields in this model [47, 50].

.....

Phys. Rev. C 87, 024914 (2013)

[47] Y. Karpenko, Y. Sinyukov, and K. Werner, (2012), arXiv:1204.5351 [nucl-th]

[50] Y. Karpenko and Y. Sinyukov, J.Phys.G **G38**, 124059 (2011).

Predictions for particle yield at LHC in central collisions

Pion, Kaon, and Proton Production in Central Pb–Pb Collisions at $\sqrt{s_{NN}}$ = 2.76 TeV

The ALICE Collaboration* **Phys. Rev. Lett. 109, 252301 (2012)**

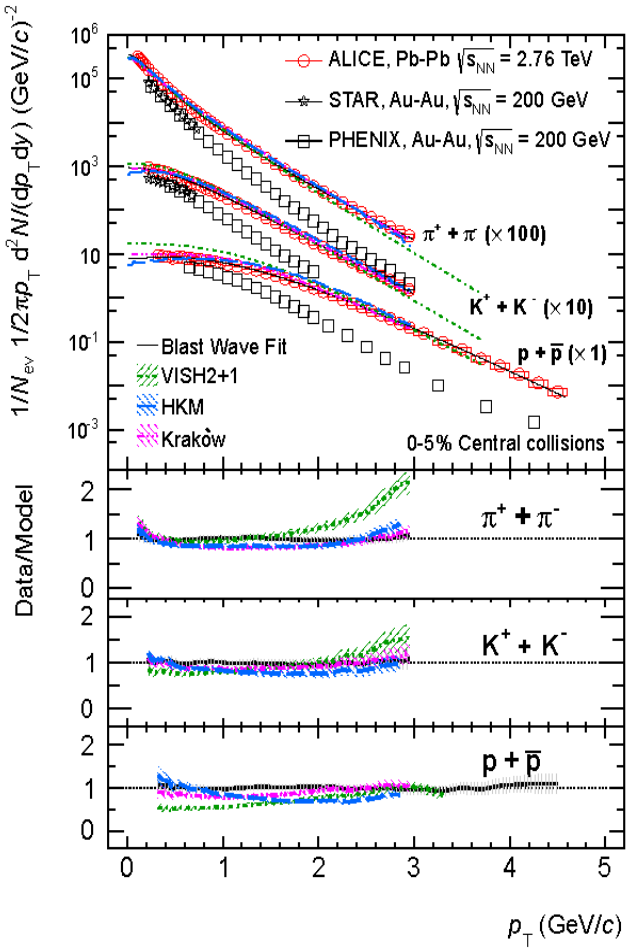

Quotations

This interpretation is supported by the comparison with HKM [39, 40], a similar model in which, after the hydrodynamic phase, particles are injected into a hadronic cascade model (UrQMD [41, 42]), which further transports them until final decoupling. The hadronic phase builds additional radial flow, mostly due to elastic interactions, and affects particle ratios due to inelastic interactions. HKM yields a better description of the data. At the LHC, hadronic final state interactions, and in particular antibaryon-baryon annihilation, may therefore be an important ingredient for the description of particle yields [43, 40], contradicting the scenario of negligible abundance-changing processes in the hadronic phase. The third model shown in Fig. 1 (Kraków [44, 45]) introduces non-equilibrium corrections due to viscosity at the transition from the hydrodynamic description to particles, which change the effective T_{ch}, leading to a good agreement with the data. In the region $p_T \lesssim 3$ GeV/c (Kraków) and $p_T \lesssim 1.5$ GeV/c (HKM) the last two models reproduce the experimental data within ~20%, supporting a hydrodynamic interpretation of the transverse momentum spectra at the LHC. These models also describe correctly other features of the space-time evolution of the system, as measured by ALICE with charged pion correlations [46].

[39] Y. Karpenko and Y. Sinyukov, J.Phys. **G38**, 124059 (2011), nucl-th/1107.3745.

[40] Y. Karpenko, Y. Sinyukov, and K. Werner, (2012), nucl-th/1204.5351.

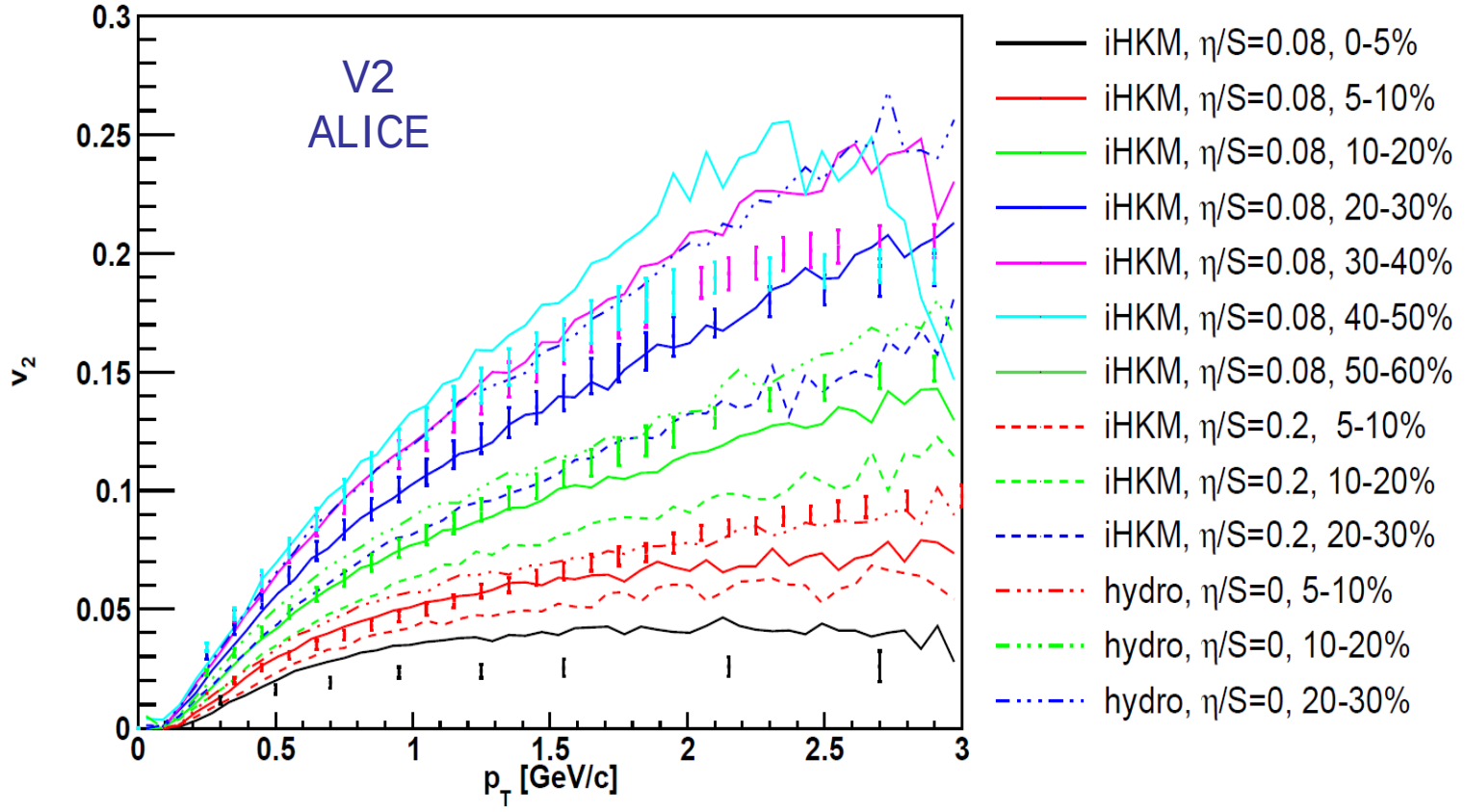

FIG. 6. All charged particles' v_2 coefficients centrality classes 0-5%, 5-10%, 10-20%, 20-30%, 30-40%, 40-50% and 50-60% obtained in the iHKM basic scenario (as in Fig. 1). The results are compared with those in iHKM at the other parameter dissipation condition, $\eta/s = 0.2$ instead of 0.08 and with ideal hydro with the starting time $\tau_{th} = \tau_0 = 0.1$ fm/c for centrality classes 5-10%, 10-20%, 20-30%. The experimental data are from [32].

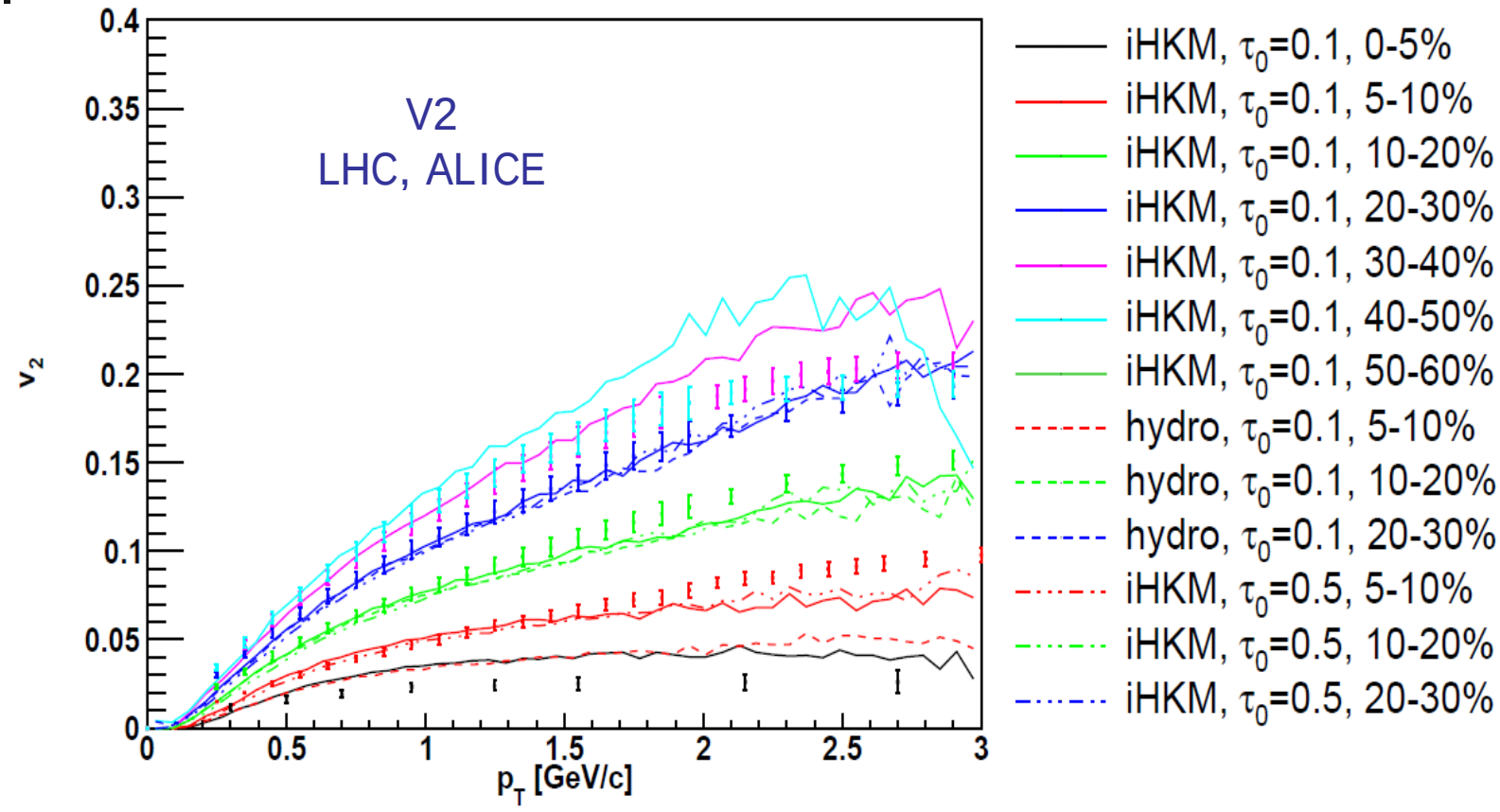

FIG. 7. All charged particles' v_2 coefficients centrality classes 0-5%, 5-10%, 10-20%, 20-30%, 30-40%, 40-50% and 50-60% obtained in the iHKM basic scenario (as in Fig. 1). The results are compared with those in iHKM at the other initial time, $\tau_0 = 0.5$ fm/c instead of 0.1 fm/c and with viscous hydro at the starting time $\tau_{th} = \tau_0 = 0.1$ fm/c for centrality classes 5-10%, 10-20%, 20-30%. The experimental data are from [32].

Important results

The $\frac{dN_{ch}}{d\eta}(c)$ is OK at fixed relative contribution of binary collision $\alpha = 0.24$.

but at different max initial energy densities when other parameters change:

The two values of the shear viscosity to entropy is used for comparison:

$$\eta/s = 0.08 \approx \frac{1}{4\pi} \text{ and } \eta/s = 0.2$$

The basic result (selected by red) is compared with results at other parameters, including viscous and ideal pure thermodynamic scenarios (starting at τ_0 without pre-thermal stage but with subsequent hadronic cascade).

Model	Λ	τ_{rel}	η/S	τ_0	$\langle \frac{\chi^2}{ndf} \rangle$	ϵ_0 (GeV/fm^3)
Hydro			0	0.1	5.16	1076.5
Hydro			0.08	0.1	6.93	738.8
iHKM	1	0.25	0.08	0.1	3.35	799.5
iHKM	100	0.25	0.08	0.1	3.68	678.8
iHKM	100	0.75	0.08	0.1	3.52	616.5
iHKM	100	0.25	0.2	0.1	6.61	596.9
iHKM	100	0.25	0.08	0.5	5.36	126.7

No dramatic worsening of the results happens if simultaneously with changing of parameters/scenarios renormalize maximal initial energy density.

The values τ_0, τ_{rel} corespond to fm/c.

Important results

The $\frac{dN_{ch}}{d\eta}(c)$ is OK at fixed relative contribution of binary collision $\alpha = 0.24$.

but at different max initial energy densities when other parameters change:

The two values of the shear viscosity to entropy is used for comparison:

$$\eta/s = 0.08 \approx \frac{1}{4\pi} \text{ and } \eta/s = 0.2$$

The basic result (selected by red) is compared with results at other parameters, including viscous and ideal pure thermodynamic scenarios (starting at τ_0 without pre-thermal stage but with subsequent hadronic cascade).

Model	Λ	τ_{rel}	η/S	τ_0	$\langle \frac{\chi^2}{ndf} \rangle$	ϵ_0 (GeV/fm^3)
Hydro			0	0.1	5.16	1076.5
Hydro			0.08	0.1	6.93	738.8
iHKM	1	0.25	0.08	0.1	3.35	799.5
iHKM	100	0.25	0.08	0.1	3.68	678.8
iHKM	100	0.75	0.08	0.1	3.52	616.5
iHKM	100	0.25	0.2	0.1	6.61	596.9
iHKM	100	0.25	0.08	0.5	5.36	126.7

No dramatic worsening of the results happens if simultaneously with changing of parameters/scenarios renormalize maximal initial energy density.

The values τ_0, τ_{rel} corespond to fm/c.

Pair femtoscopic correlations: Bose-Einstein/Fermi-Dirac + final state interactions (BE/FD + FSI)

$$C(p,q) = 1 + \lambda \frac{\int d^4x_1 d^4x_2 g_1(x_1,p) g_2(x_2,p) \left(|\psi(\tilde{q},r)|^2 - 1 \right)}{\int d^4x_1 g_1(x_1,p_1) \int d^4x_2 g_2(x_2,p_2)} = 1 + \lambda \left\langle \left(|\psi(\tilde{q},r)|^2 - 1 \right) \right\rangle$$

where $\psi(\tilde{q},r)$ is reduced Bether-Salpeter amplitude, $r = x_1 - x_2, R = (x_1 + x_2)/2$

$$q = p_1 - p_2, p = (p_1 + p_2)/2 \qquad \tilde{q} = q - p(qp)/p^2$$

Pair femtoscopic correlations: Bose-Einstein/Fermi-Dirac + final state interactions (BE/FD + FSI)

$$C(p,q) = 1 + \lambda \frac{\int d^4x_1 d^4x_2 g_1(x_1,p) g_2(x_2,p) \left(|\psi(\tilde{q},r)|^2 - 1 \right)}{\int d^4x_1 g_1(x_1,p_1) \int d^4x_2 g_2(x_2,p_2)} = 1 + \lambda \left\langle \left(|\psi(\tilde{q},r)|^2 - 1 \right) \right\rangle$$

where $\psi(\tilde{q},r)$ is reduced Bether-Salpeter amplitude, $r = x_1 - x_2, R = (x_1 + x_2)/2$

$$q = p_1 - p_2, p = (p_1 + p_2)/2 \qquad \tilde{q} = q - p(qp)/p^2$$

For identical bosons (in smoothness approximation) with only Coulomb FSI

Y. Sinyukov, R. Lednicky, S.V. Akkelin, J. Pluta, B. Erazmus, Phys. Lett. B 432 (1998) 248.

$$C(p,q) = 1 - \lambda + \lambda \left\langle \left| \psi^c_{-\mathbf{k}*}(\mathbf{r}^*) \right|^2 \right\rangle (1 + \langle \cos(qx) \rangle) \rightarrow 1 + \lambda \langle \cos(qx) \rangle$$

$$\mathbf{k}^* = \mathbf{q}^*/2$$

where $\langle \cos(qx) \rangle = \exp(-q_{out}^2 R_{out}^2 - q_{side}^2 R_{side}^2 - q_{long}^2 R_{long}^2 - ...c.t.)$ $\qquad \mathbf{r}* = \mathbf{x}_1^* - \mathbf{x}_2^*$

Pair femtoscopic correlations: Bose-Einstein/Fermi-Dirac + final state interactions (BE/FD + FSI)

$$C(p,q) = 1 + \lambda \frac{\int d^4x_1 d^4x_2 g_1(x_1,p) g_2(x_2,p) \left(|\psi(\tilde{q},r)|^2 - 1 \right)}{\int d^4x_1 g_1(x_1,p_1) \int d^4x_2 g_2(x_2,p_2)} = 1 + \lambda \left\langle \left(|\psi(\tilde{q},r)|^2 - 1 \right) \right\rangle$$

where $\psi(\tilde{q},r)$ is reduced Bether-Salpeter amplitude, $r = x_1 - x_2, R = (x_1 + x_2)/2$

$$q = p_1 - p_2, p = (p_1 + p_2)/2 \qquad \tilde{q} = q - p(qp)/p^2$$

For identical bosons (in smoothness approximation) with only Coulomb FSI

Y. Sinyukov, R. Lednicky, S.V. Akkelin, J. Pluta, B. Erazmus, Phys. Lett. B 432 (1998) 248.

$$C(p,q) = 1 - \lambda + \lambda \left\langle \left| \psi^c_{-\mathbf{k}*}(\mathbf{r}^*) \right|^2 \right\rangle (1 + \langle \cos(qx) \rangle) \rightarrow 1 + \lambda \langle \cos(qx) \rangle$$

$$\mathbf{k}^* = \mathbf{q}^*/2$$

where $\langle \cos(qx) \rangle = \exp(-q^2_{out} R^2_{out} - q^2_{side} R^2_{side} - q^2_{long} R^2_{long} - ...c.t.)$ $\qquad \mathbf{r}* = \mathbf{x}^*_\mathbf{1} - \mathbf{x}^*_\mathbf{2}$

Correlation functions in semi-classical events generators BE correlation:

$$C(\vec{q}) = \frac{\sum_{i \neq j} \delta_\Delta(\vec{q} - p_i + p_j)(1 + cos(p_j - p_i)(x_j - x_i))}{\sum_{i \neq j} \delta_\Delta(\vec{q} - p_i + p_j)}$$

where $\delta_\Delta(x) = 1$ if $|x| < \Delta p/2$ and 0 otherwise, with Δp being the bin size in histograms.

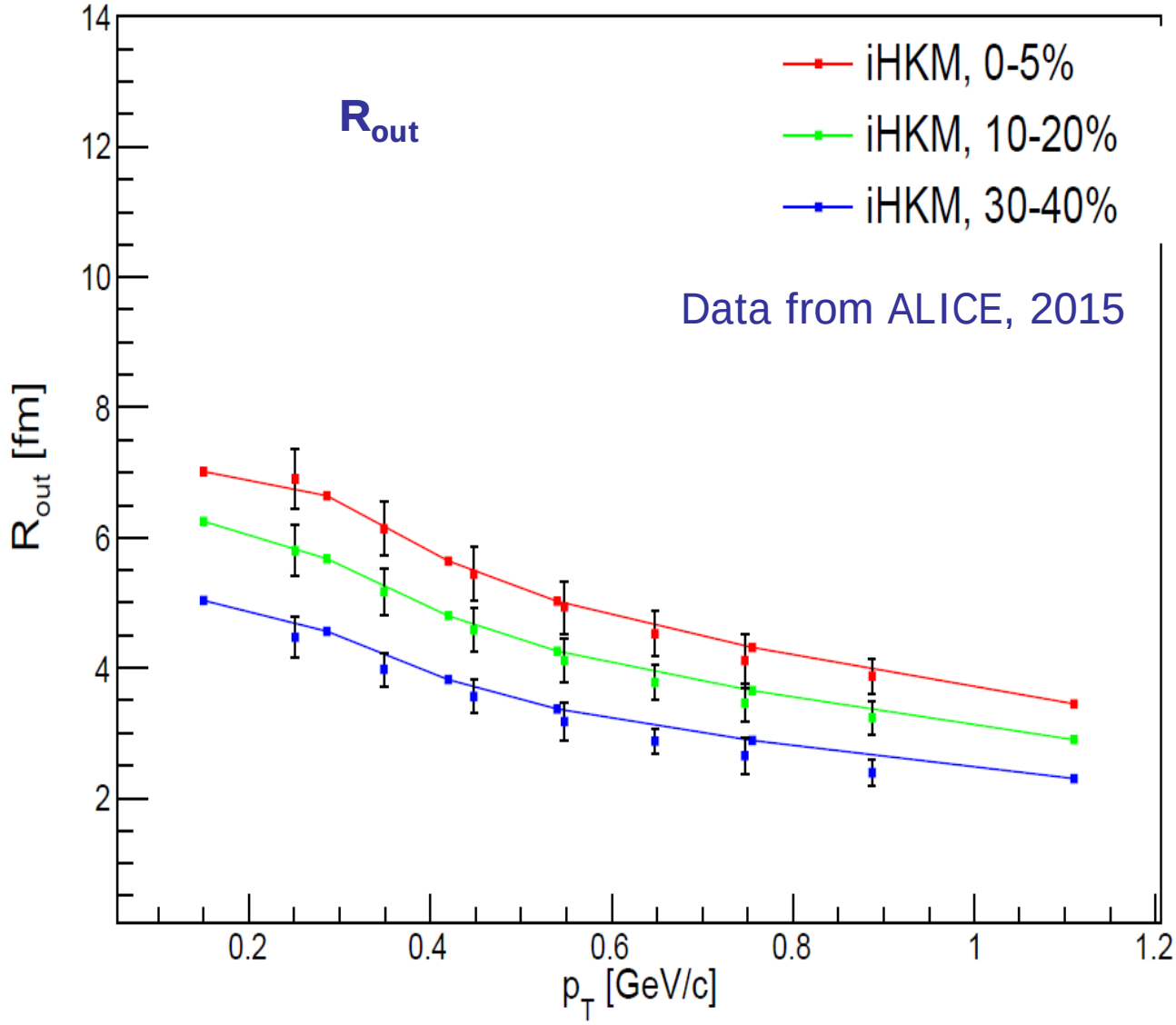

FIG. 8. The R_{out} dependence on transverse momentum for different centralities in the iHKM basic scenario under the same conditions as in Fig. 1.

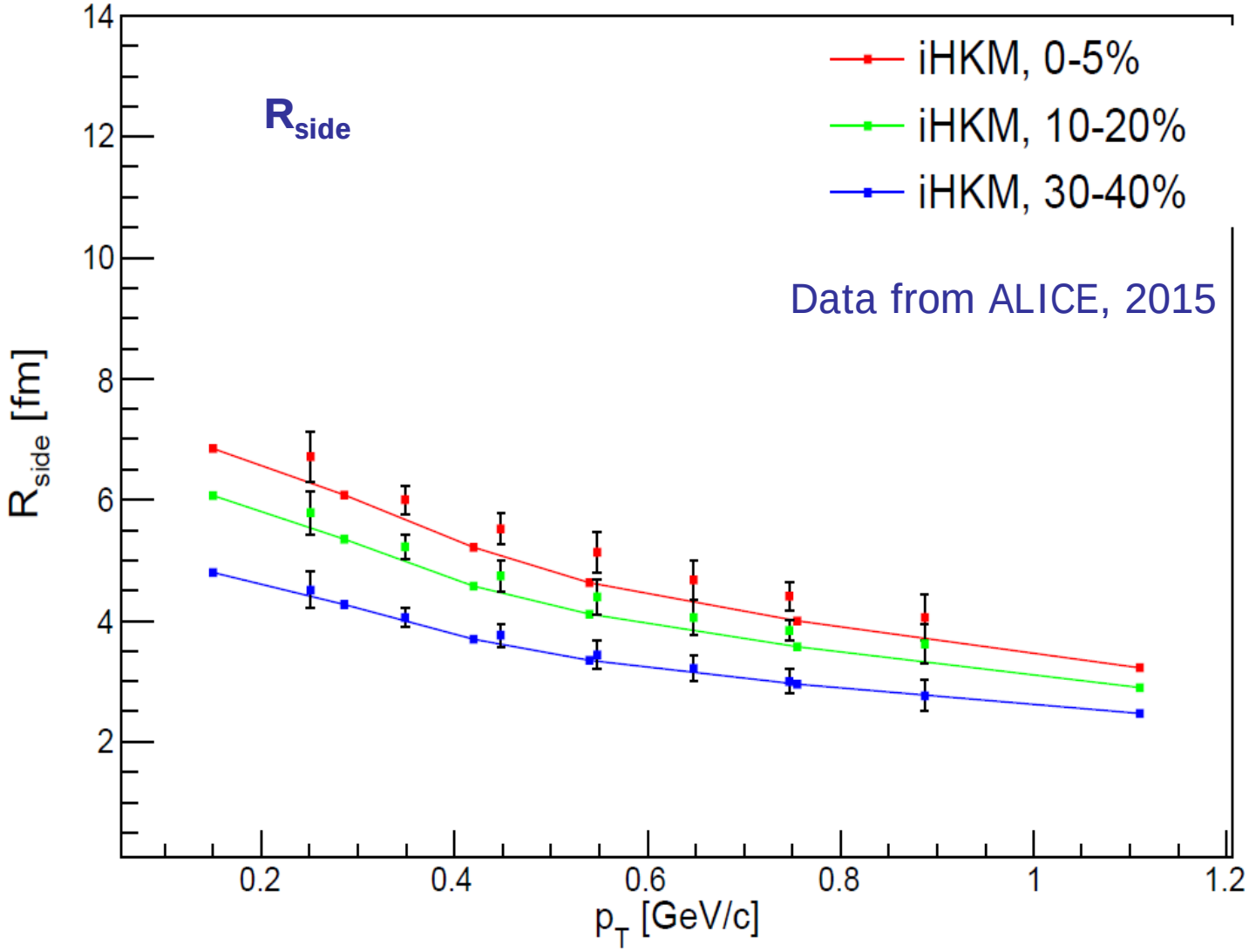

FIG. 9. The R_{side} dependence on transverse momentum for different centralities in the iHKM scenario under the same conditions as in Fig. 1. The experimental data are from [33].

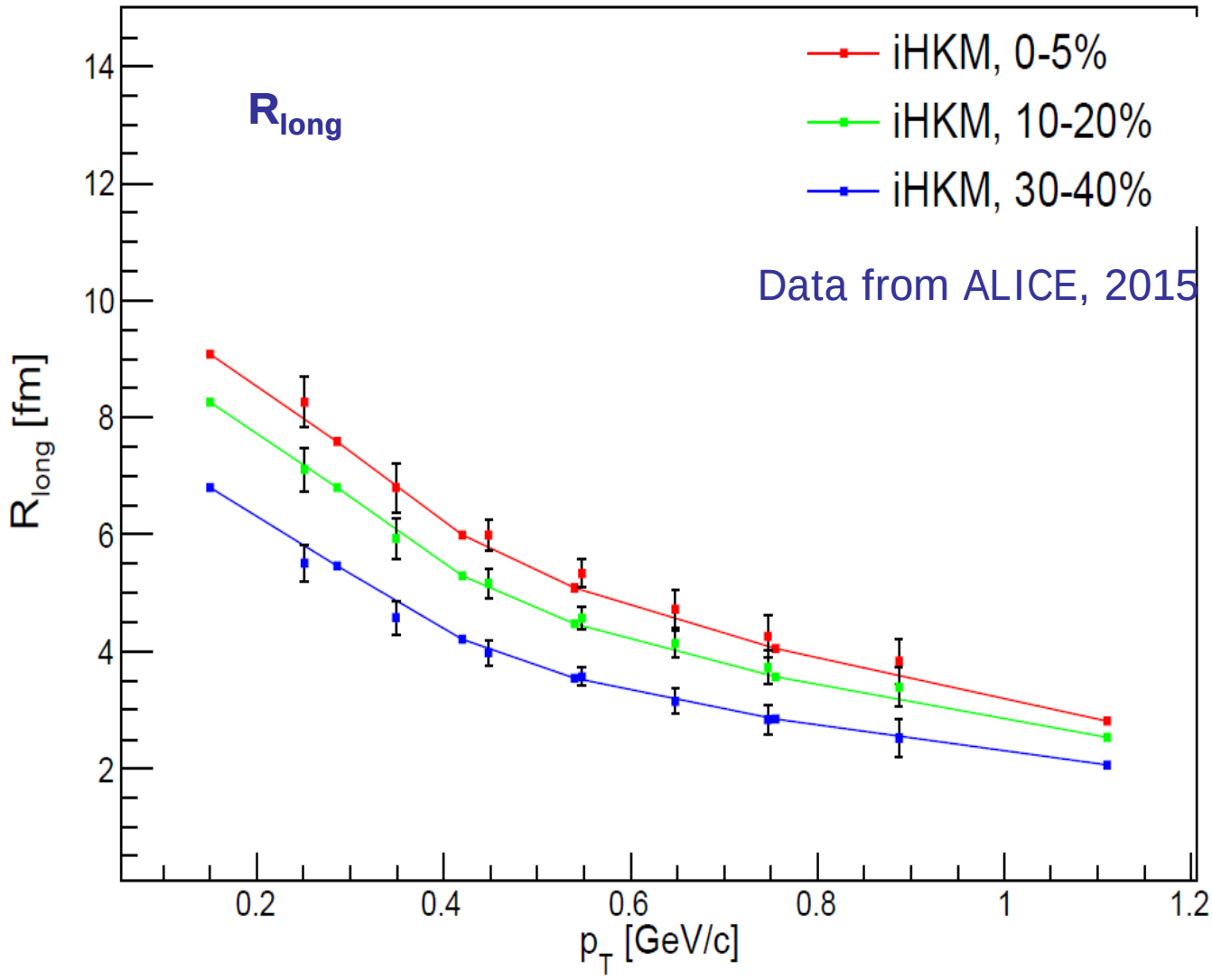

FIG. 10. The R_{long} dependence on transverse momentum for different centralities in the iHKM basic scenario - the same conditions as in Fig. 1. The experimental data are from [33].

$K^{\pm}K^{\pm}$ and $K^0_s K^0_s$ in Pb-Pb: HKM model

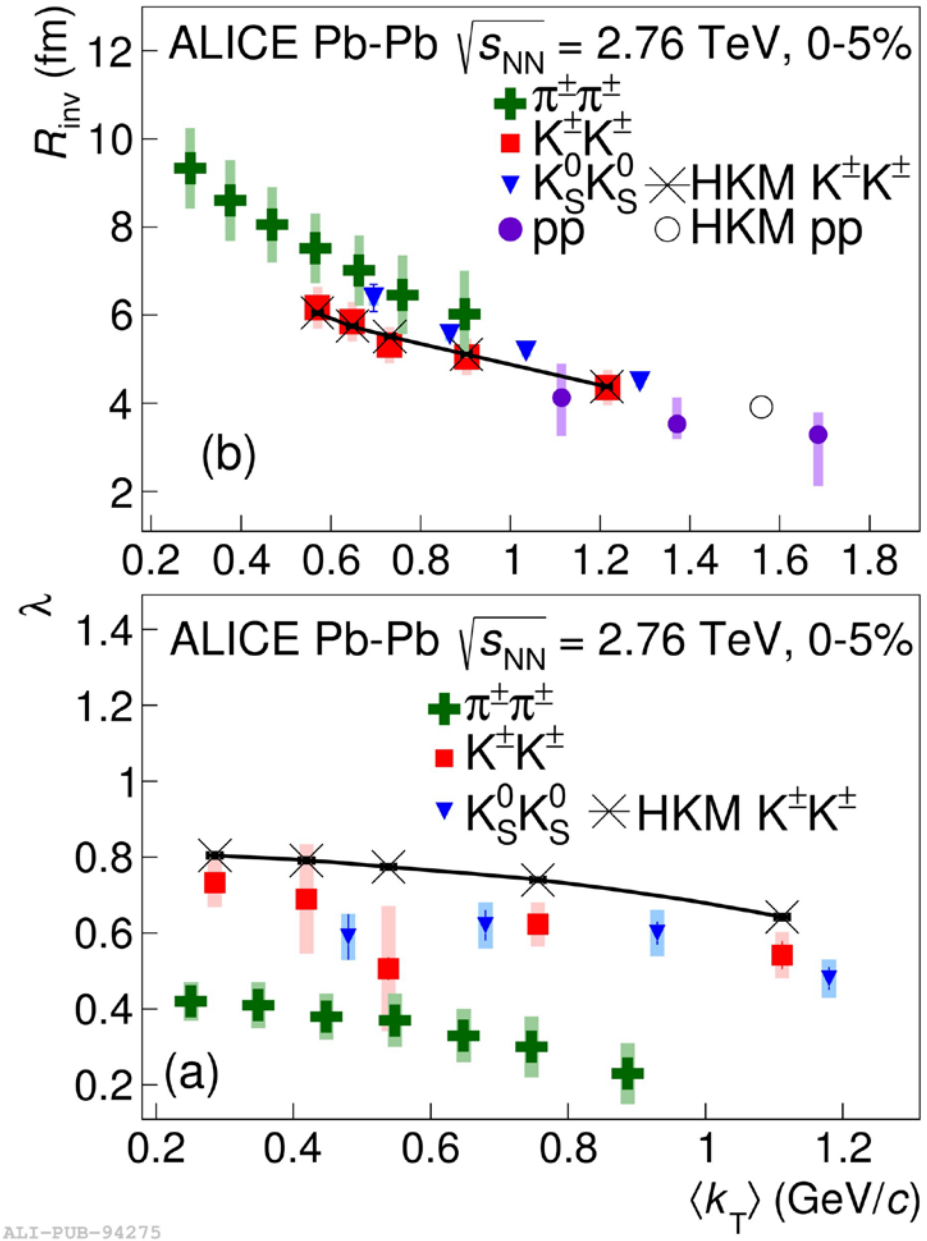

New results from ArXiv.org:1506.07884

- R and λ for $\pi^{\pm}\pi^{\pm}$, $K^{\pm}K^{\pm}$, $K^0_s K^0_s$, pp for 0-5% centrality
- Radii for kaons show good agreement with HKM predictions for $K^{\pm}K^{\pm}$ (V. Shapoval, P. Braun-Munzinger, Yu. Sinyukov Nucl.Phys.A929 (2014))

- λ decrease with k_T, both data and HKM
- HKM prediction for λ slightly overpredicts the data
- Λ_π are lower λ_K due to the stronger influence of resonances

Comparison with HKM for 0-5% centrality

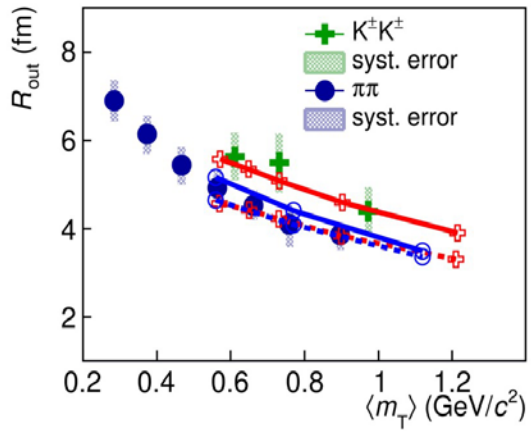

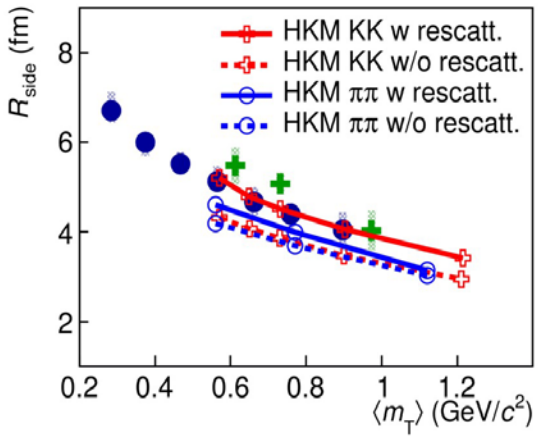

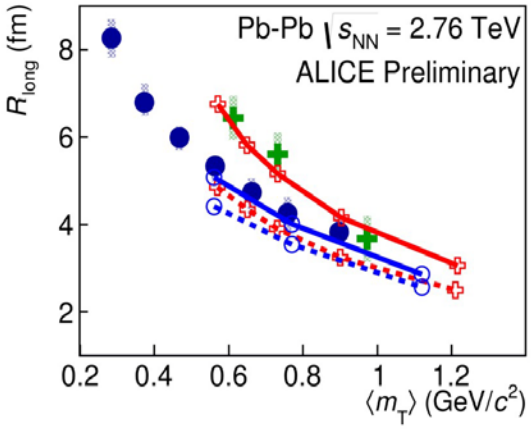

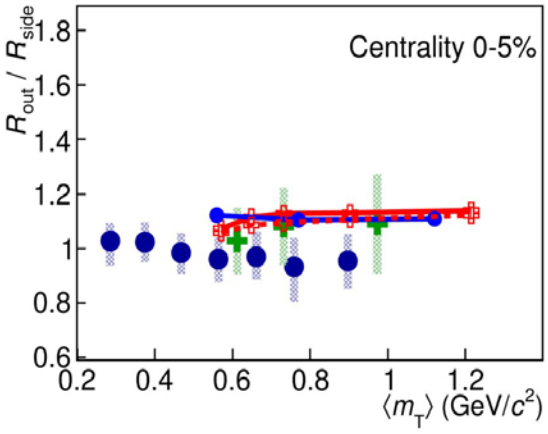

ALI-PREL-96575

- HKM model slightly underestimates R_{side} → overestimates R_{out}/R_{side} ratio for π

- HKM model with re-scatterings (M. Shapoval, P. Braun-Munzinger, Iu.A. Karpenko, Yu.M. Sinyukov, Nucl.Phys. A 929 (2014) 1.) describes well ALICE π & K data.

- HKM model w/o re-scatterings demonstrates approximate m_T scaling for π & K, but does not describe ALICE π & K data

- The observed deviation from m_T scaling is explained in (M. Shapoval, P. Braun-Munzinger, Iu.A. Karpenko, Yu.M. Sinyukov, Nucl.Phys. A 929 (2014) by essential transverse flow & re-scattering phase.

3D $K^{\pm}K^{\pm}$ & $\pi\pi$ radii versus k_T

Pion results from ArXiv.org:1507.06842

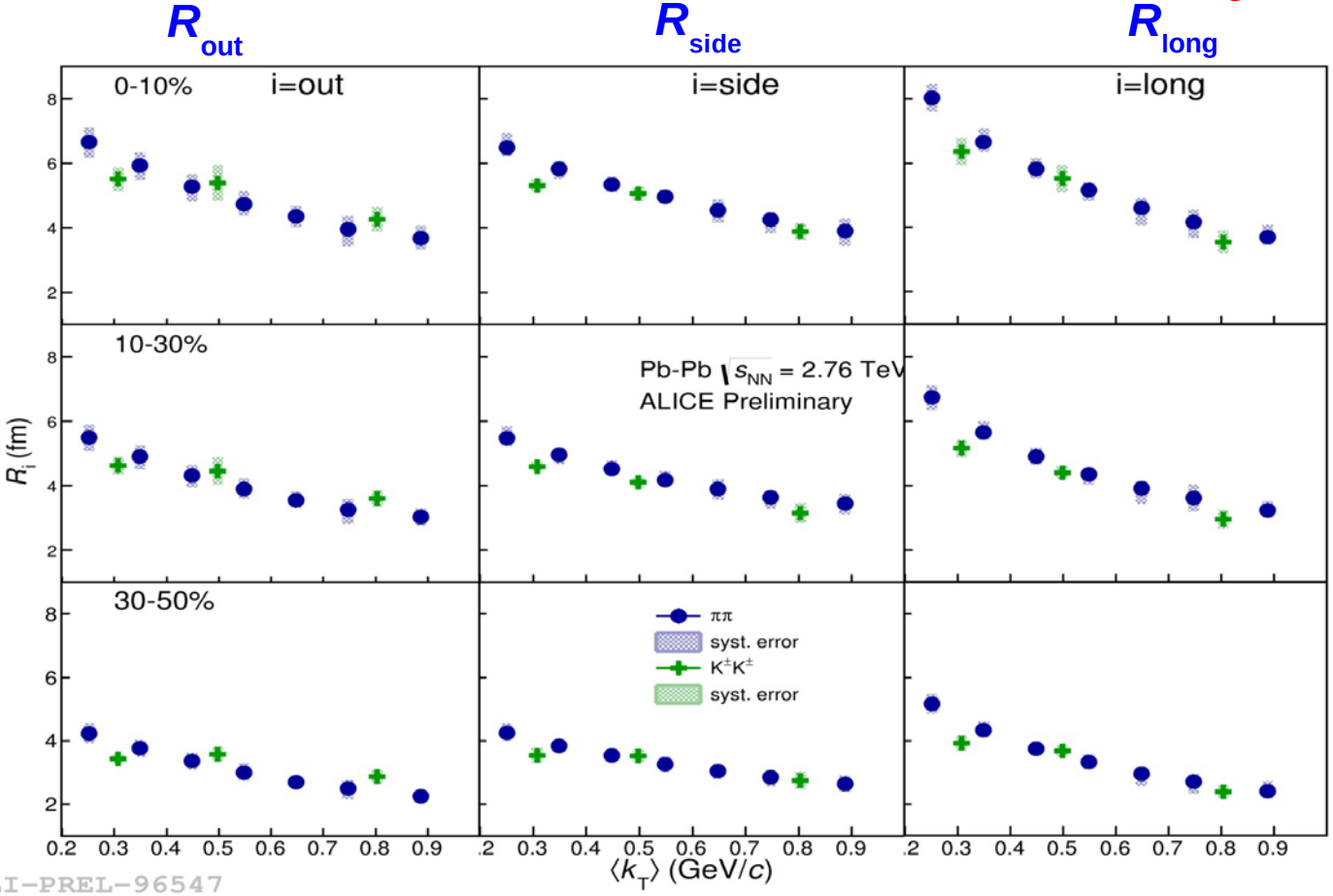

- Radii scale better with k_T than with m_T according with HKM predictions (V. Shapoval, P. Braun-Munzinger, Iu.A. Karpenko, Yu.M. Sinyukov, Nucl.Phys. A 929 (2014) 1);
- Similar observations were reported by PHENIX at RHIC (arxiv:1504.05168).

Extraction of emission time from fit R_{long} $T_{\perp}^{2}(m_{\perp})$

- The new formula for extraction of the maximal emission time for the case of strong transverse flow was used (Yu. Sinyukov, V.Shapoval, V.Naboka, arXiv:1508.01812)

- The parameters of freeze-out: T and "intensity of transverse flow" α were fixed by fitting π and K spectra (arxiv:1508.01812)

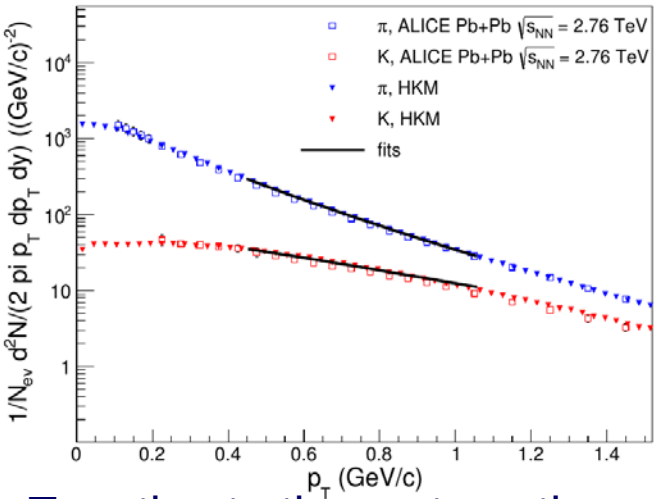

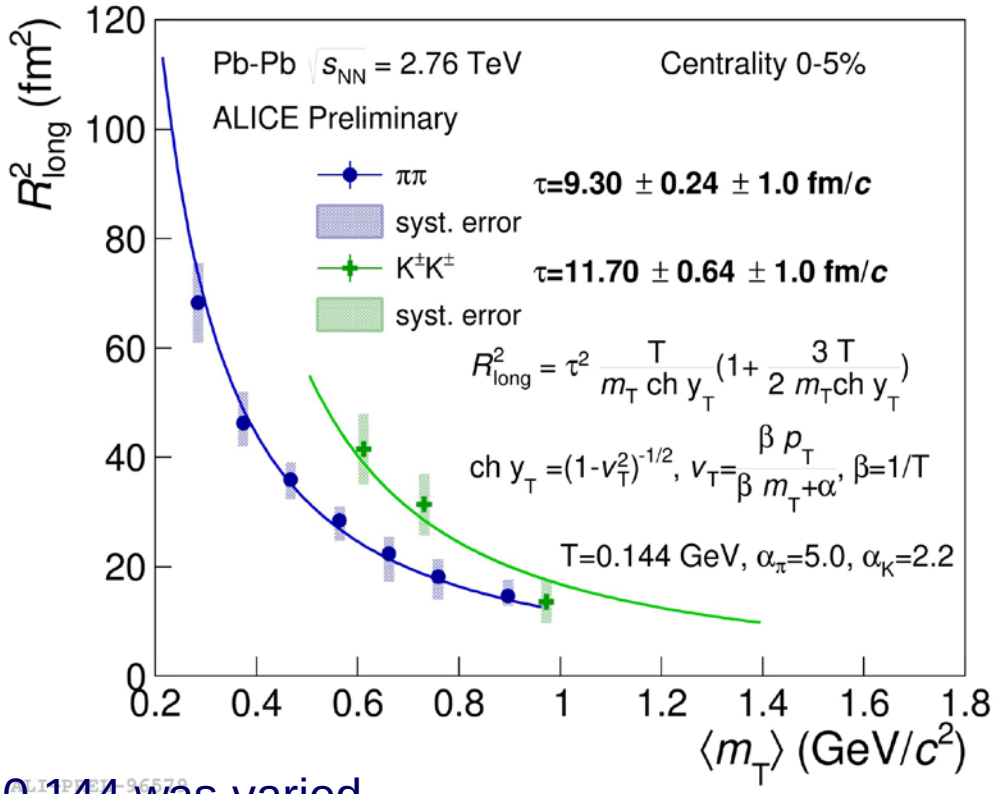

- To estimate the systematic errors: T = 0.144 was varied on ± 0.03 GeV & free α_π, α_K, were used; systematic errors ~ 1 fm/c

- Indication: $\tau_\pi < \tau_K$. Possible explanations (arxiv:1508.01812): HKM includes re-scatterings (UrQMD cascade): e.g. Kπ→K*(892)→Kπ, KN→K*(892)X; (K*(892) lifetime 4-5 fm/c) [πN→N*(Δ)X, N*(Δ)→πX (N*s(Δs)- short lifetime)]

Space-time picture of the pion and kaon emission

$$\underbrace{R_l^2(k_T) = \tau^2\lambda^2\left(1+\frac{3}{2}\lambda^2\right)}_{\text{2015}} \approx \text{w/o transv. expansion} \approx \underbrace{\tau^2\frac{T}{m_T}}_{\text{1987}}\underbrace{\frac{K_2(\frac{m_T}{T})}{K_1(\frac{m_T}{T})}}_{\text{1995}}$$

where $\lambda^2 = \frac{T}{m_T}\left(1-\frac{\overbrace{k_T^2}^{\bar{v}_T^2}}{(m_T+\alpha T)^2}\right)^{1/2}$

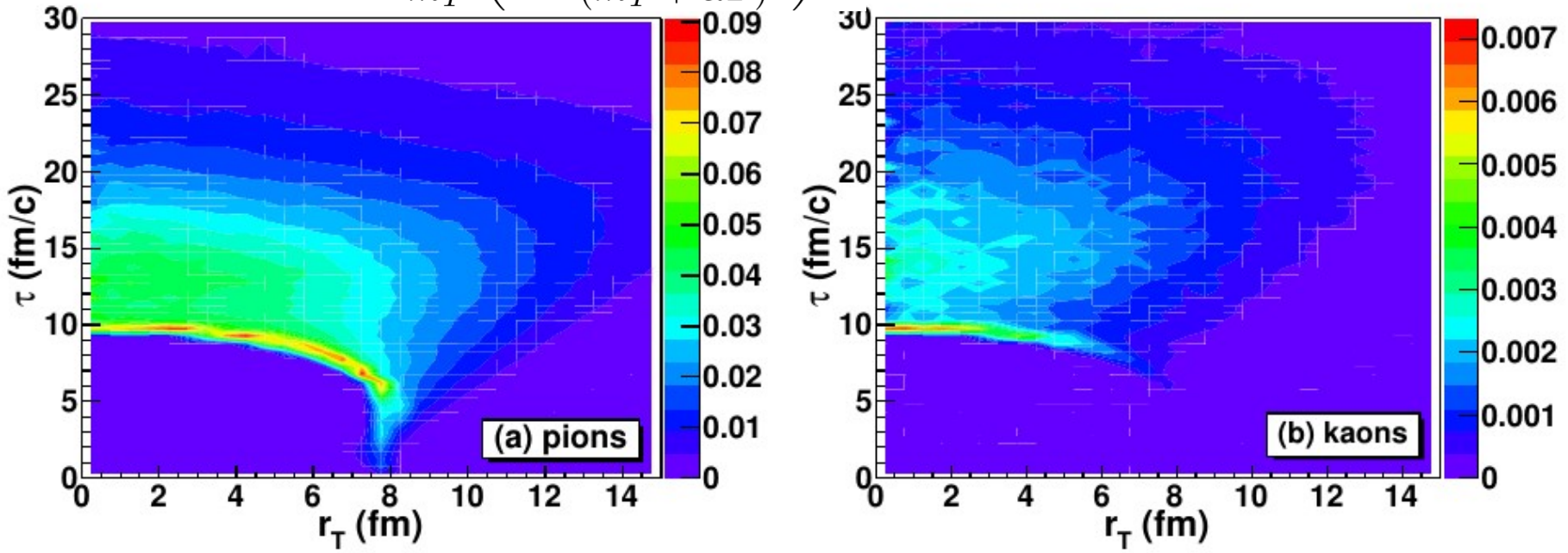

FIG. 4. The momentum angle averaged emission functions per units of space-time and momentum rapidities $g(\tau, r_T, p_T)$ [fm^{-3}] (see body text) for pions (a) and kaons (b) obtained from the HKM simulations of Pb+Pb collisions at the LHC $\sqrt{s_{NN}} = 2.76$ GeV, $0.2 < p_T < 0.3$ GeV/c, $|y| < 0.5$, $c = 0-5\%$. From Yu.S., Shapoval, Naboka, Nucl. Phys. A 946 (2016) 247 (arXiv:1508.01812)

The K(892)* production and its decay in hadronic medium at the LHC (Shapoval, Braun-Munzinger, Yu.S., 2016)

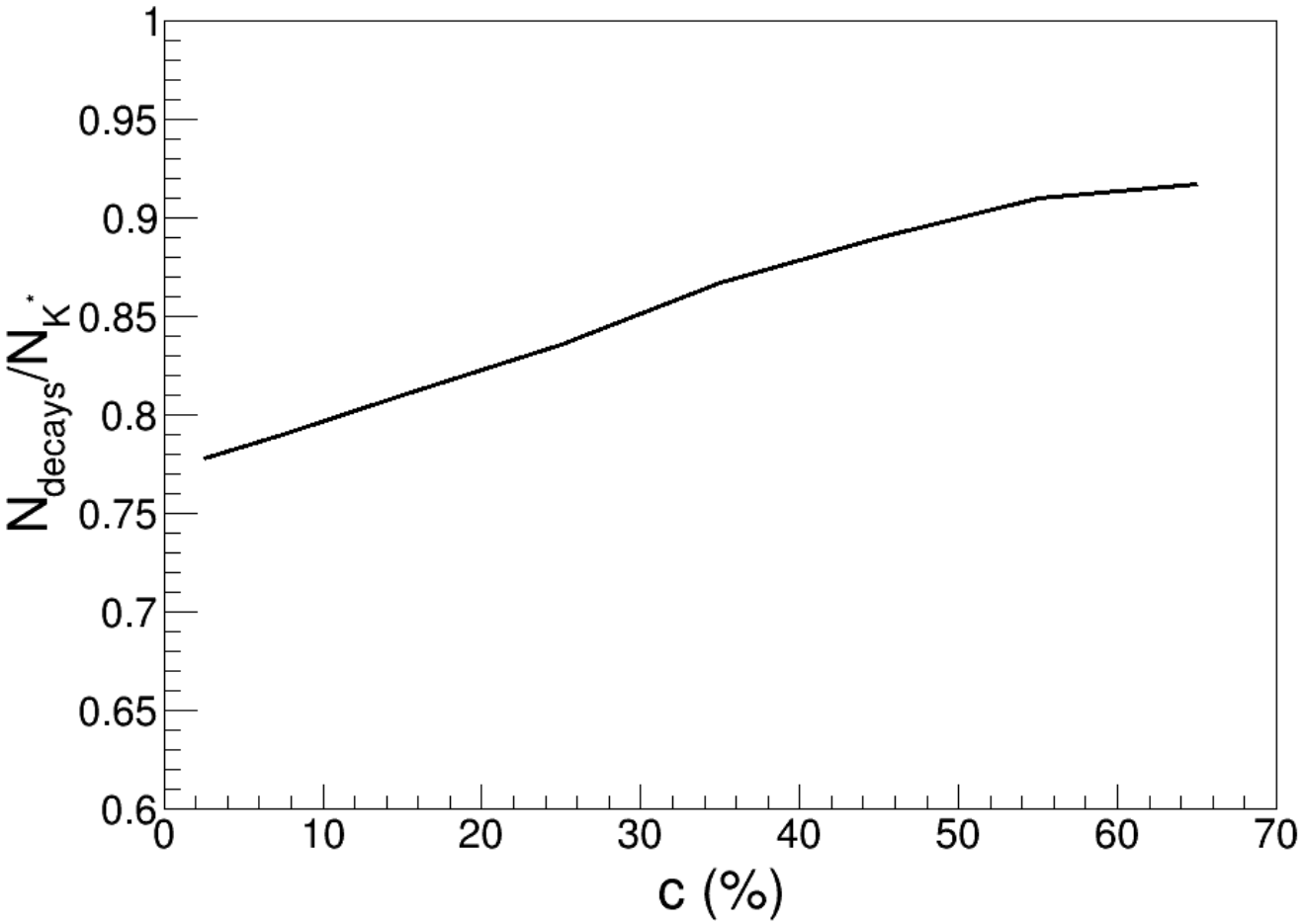

The fraction of $K^+\pi^-$ pairs coming from $K(892)^*$ decay, which can be identified as K^* daughters in iHKM simulations after the particle rescattering stage modeled within UrQMD hadron cascade. The simulations correspond to LHC Pb+Pb collisions at $\sqrt{s_{NN}} = 2.76$ TeV with different centralities.

K*/K ratio vs centrality

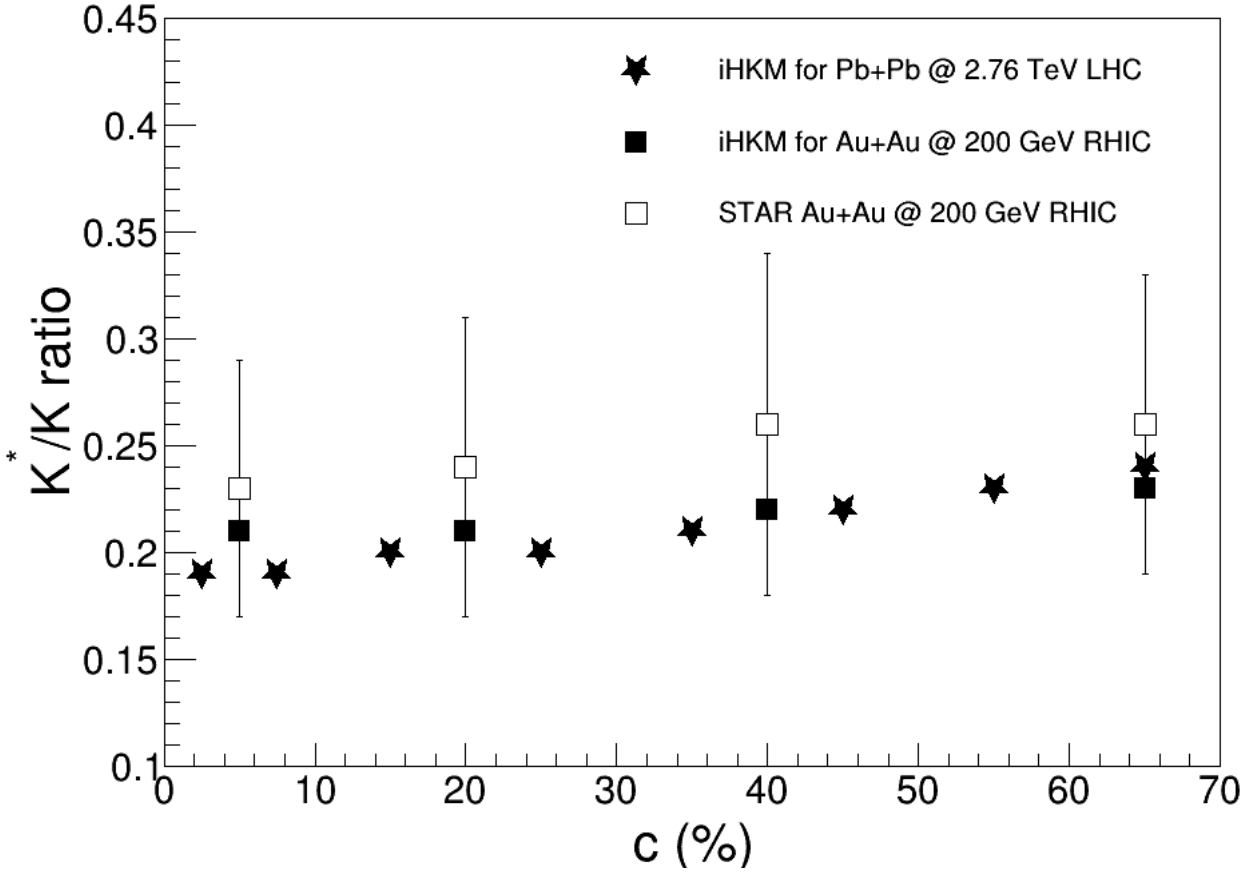

The comparison of K^*/K^+ ratio calculated in iHKM for the case of RHIC Au+Au collisions at $\sqrt{s_{NN}} = 200$ GeV and the experimental data [7] for different centrality classes.

Prediction for LHC Pb+Pb collisions at $\sqrt{s_{NN}} = 2.76$ TeV

Source function S(r*)

Integrated in time distribution of the pairs on relative distance between particles in the pairs in the rest frames of the pairs

The correlation function in smoothness approximation

$$C(p,q) = 1 + \frac{\int d^4x_1 d^4x_2 g_1(x_1,p_1) g_2(x_2,p_2) \left(|\psi(\tilde{q},r)|^2 - 1 \right)}{\int d^4x_1 g_1(x_1,p_1) \int d^4x_2 g_2(x_2,p_2)}$$

where $\psi(\tilde{q},r)$ is reduced Bether-Salpeter amplitude, $r = x_1 - x_2, R = (x_1+x_2)/2$

$$q = p_1 - p_2, p = (p_1+p_2)/2 \qquad \tilde{q} = q - p(qp)/p^2$$

The relative distance distribution function

$$s(r,p_1,p_2) = \frac{\int d^4R g_1(R+r/2,p_1) g_2(R-r/2,p_2)}{\int d^4R g_1(R,p_1) \int d^4R g_2(R,p_2)} =$$

Main contribution to $C(p_1,p_2)$ is at $\mathbf{v}_1 \approx \mathbf{v}_2$

$$= \int d^4R \tilde{g_1}(R+r/2, \frac{2m_1}{m_1+m_2}p) \tilde{g_2}(R-r/2, \frac{2m_2}{m_1+m_2}p) = s(r,p)$$

$$\overbrace{C(\mathbf{q}^*, \mathbf{p}{=}\mathbf{0}) - 1}^{R(\mathbf{q})} = \int d^3r^* \int \underbrace{dt^* s(r^*,\mathbf{0})}_{S(\mathbf{r}^*)} (|\psi(\mathbf{r}^*,\mathbf{q}^*)|^2 - 1) = \int d^3r^* S(\mathbf{r}^*) K(\mathbf{r}^*,\mathbf{q}^*)$$

m_T scaling of source radii for meson and baryon pairs because in pair rest frame the transverse flow are absent

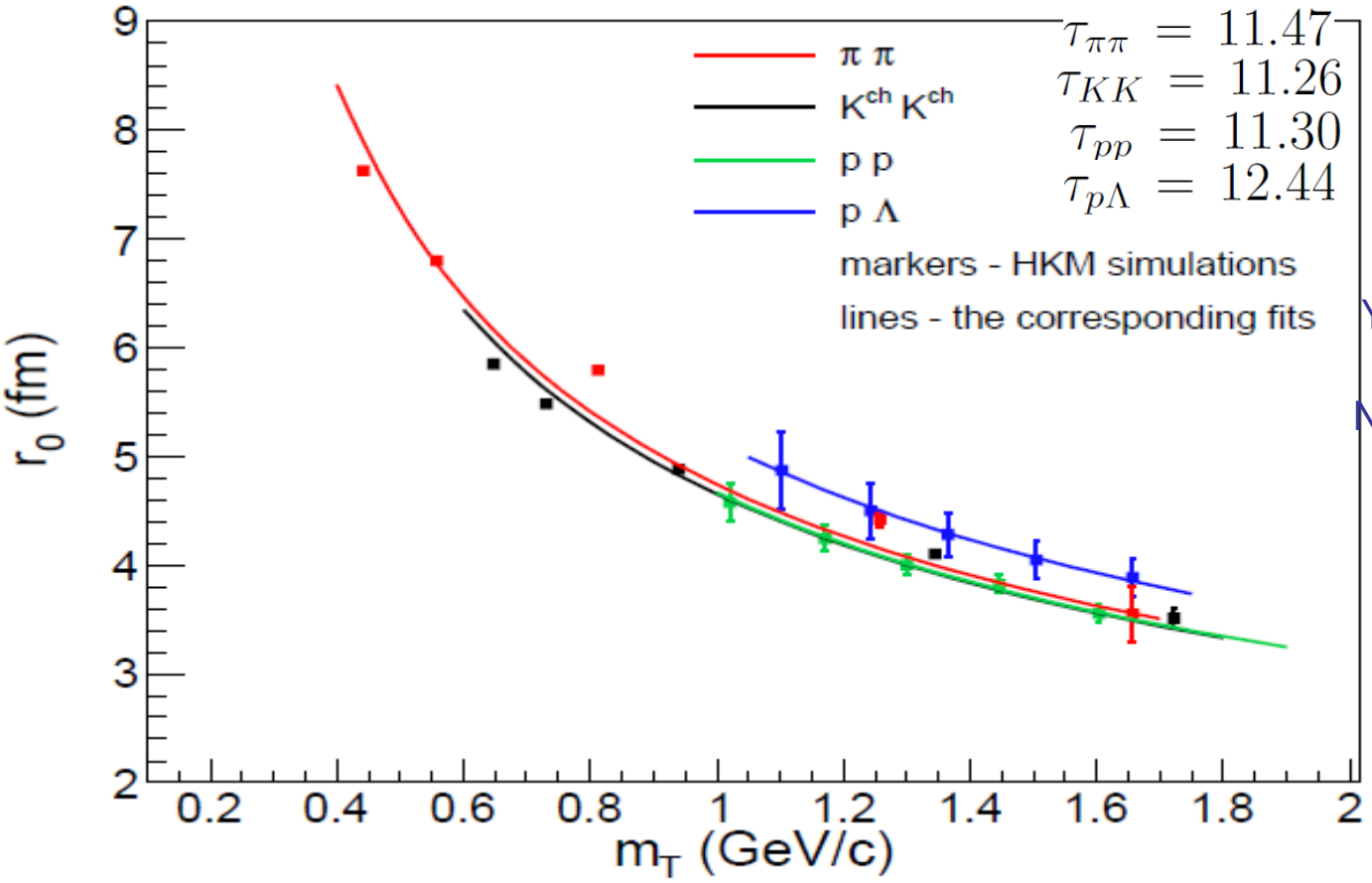

Yu.S., Shapoval, Naboka, Nucl. Phys. A 946 (2016) 247

FIG. 7. The m_T dependencies of $\pi\pi$, $K^{ch}K^{ch}$, pp and $p\Lambda$ source radii r_0 extracted from corresponding angle-averaged source functions calculated in HKM for $\sqrt{s_{NN}} = 2.76$ GeV Pb+Pb collisions at the LHC, $c = 0 - 5\%$, $|\eta| < 0.8$. Transverse momentum ranges are $0.14 < p_T < 1.5$ GeV/c for pions and kaons, $0.7 < p_T < 4.0$ GeV/c for protons and $0.7 < p_T < 5.0$ GeV/c for Lambdas.

The $p-\Lambda \oplus \bar{p}-\bar{\Lambda}$ correlation function RHIC

F. Wang, S. Pratt, Phys. Rev. Lett. 83, 3138 (1999)

$f_0^s = 2.88$ fm, $f_0^t = 1.66$ fm, $d_0^s = 2.92$ fm, $d_0^t = 3.78$ fm

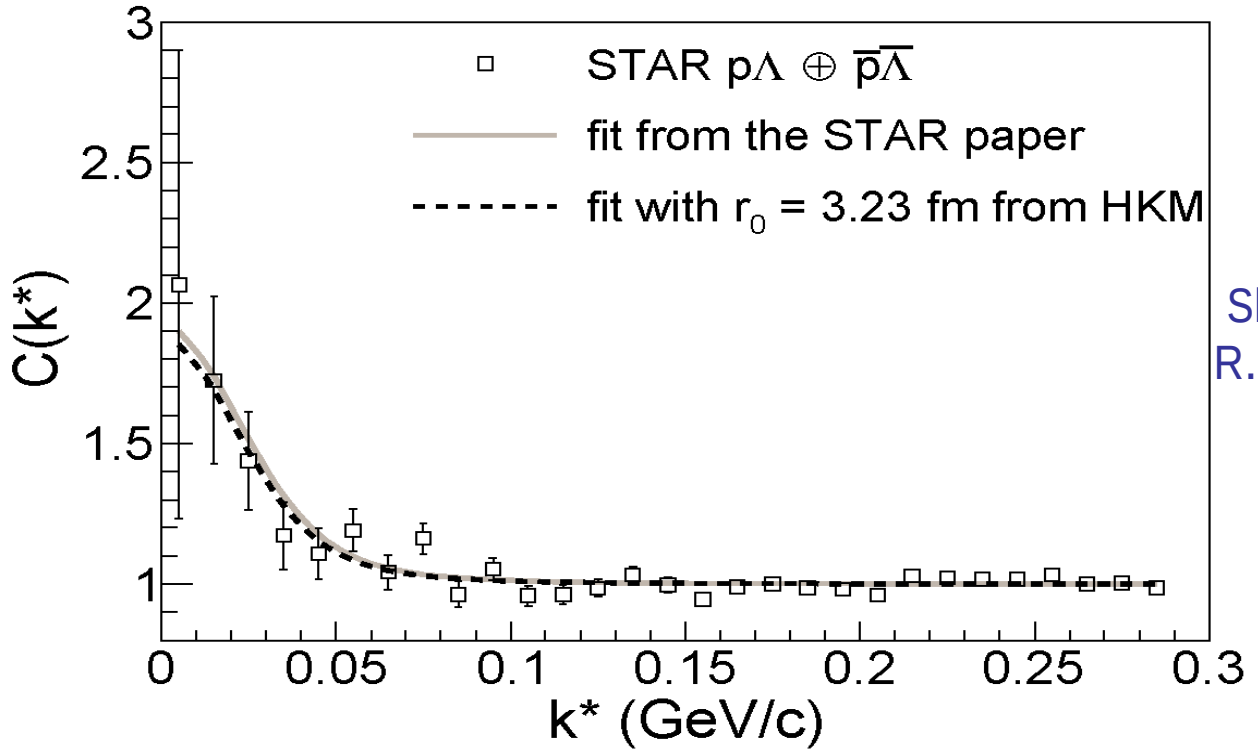

Shapoval, Erazmus, R. Lednicky, and Yu.S. Phys. Rev. C **92**, 034910 (2015)

The $p-\Lambda \oplus \bar{p}-\bar{\Lambda}$ correlation function measured by STAR (open markers), the corresponding fit according to (6) with parameters fixed as in the STAR paper [4] within the Lednický and Lyuboshitz analytical model [1] (light solid line) and our fit within the same model with the source radius r_0 extracted from the HKM calculations (dark dashed line).

The $\bar{p}-\Lambda \oplus p-\bar{\Lambda}$ correlation function RHIC

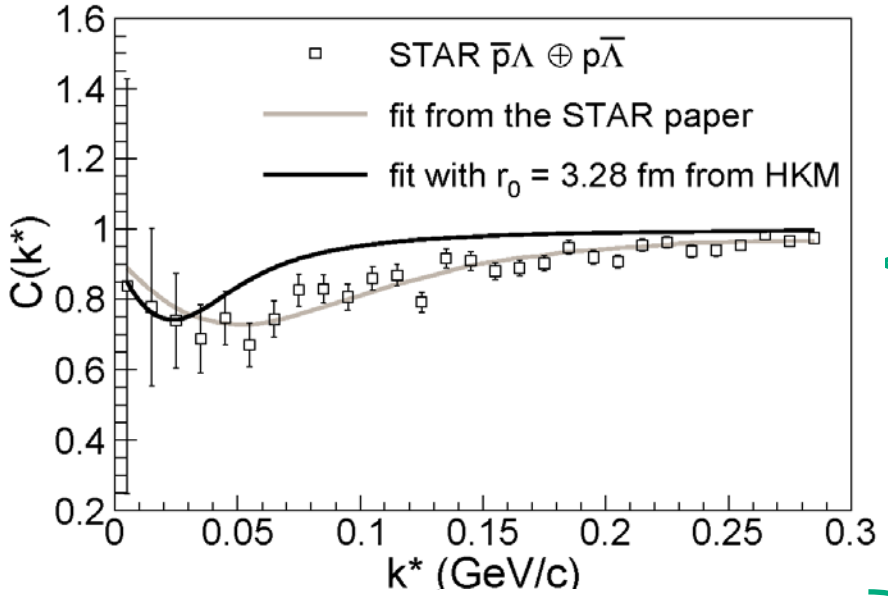

$$\text{STAR: } \Re f = -2.03 \pm 0.96^{+1.37}_{-0.12} \text{ fm},$$
$$\Im f = 1.01 \pm 0.92^{+2.43}_{-1.11} \text{ fm},$$
$$r_0 = 1.50 \pm 0.05^{+0.10}_{-0.12} \pm 0.3 \text{ fm}$$

$$C_{meas}(k^*) = \lambda(k^*)C(k^*) + (1-\lambda(k^*))$$

Residual correlations

$$C_{uncorr}(k^*) = 1 + \lambda(k^*)(C(k^*)-1) + \alpha(k^*)(C_{res}(k^*)-1)$$

$$C_{res}(k^*) = 1 - \tilde{\beta} e^{-4k^{*2}R^2}$$

$$\Re f_0 = 0.14 \pm 0.66 \text{ fm},$$

$$\Im f_0 = 1.53 \pm 1.31 \text{ fm}, \ \beta = 0.034 \pm 0.005$$

and $R = 0.48 \pm 0.05$ fm, with $\chi^2/\text{ndf} = 0.87$.

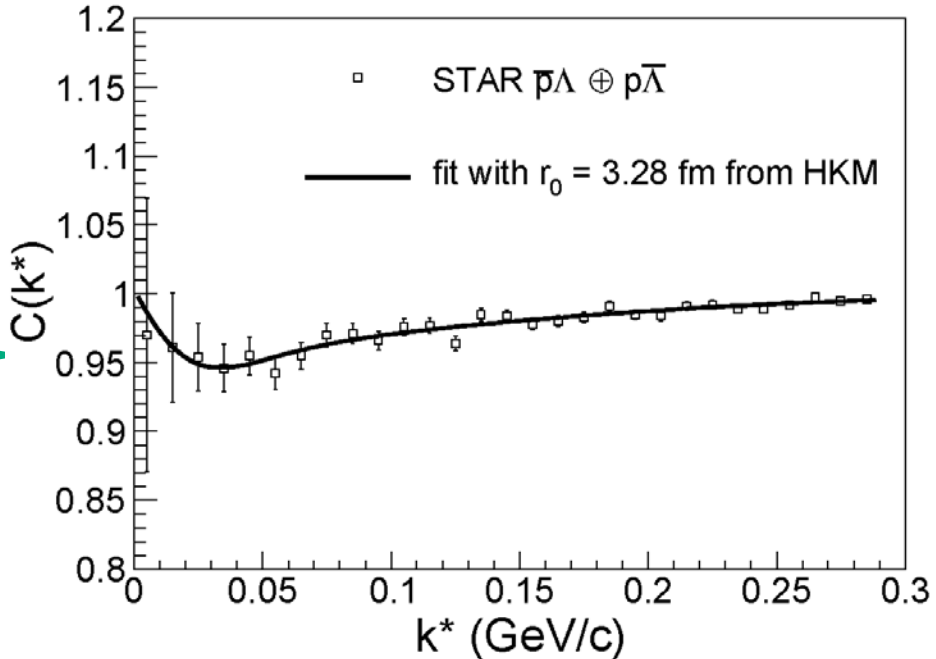

The $p-\Lambda \oplus \bar{p}-\bar{\Lambda}$ correlation function (prediction for LHC)

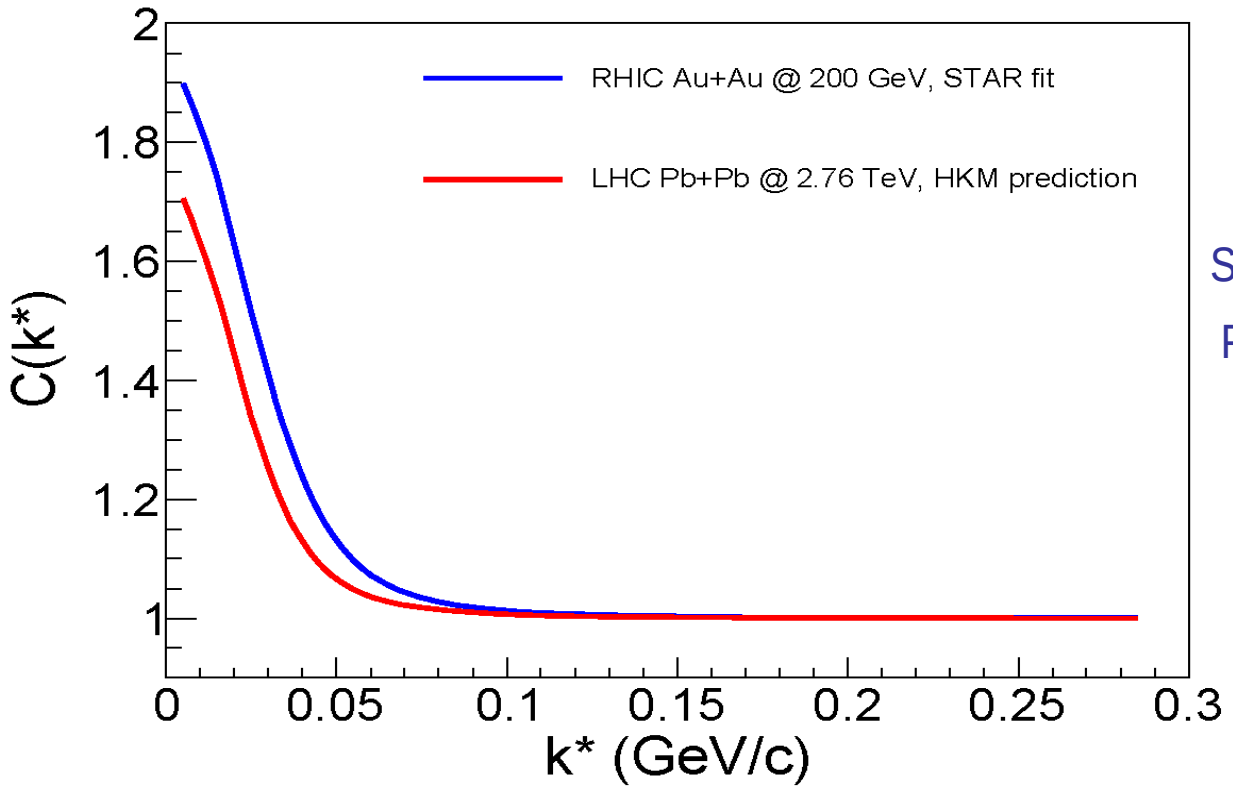

Shapoval, Yu. S. ,Naboka

Phys. Rev. C **92**, 044910 (2015)

FIG. 2. The HKM prediction for purity corrected $p-\Lambda \oplus \bar{p}-\bar{\Lambda}$ correlation function in the LHC Pb+Pb collisions at $\sqrt{s_{NN}} = 2.76$ TeV, $c = 0-5\%$, $|\eta| < 0.8$, with $0.7 < p_T < 4$ GeV/c for protons and $0.7 < p_T < 5$ GeV/c for lambdas (red line). The LHC source radius value calculated in HKM is $r_0 = 3.76$ fm. The Lednický-Lyuboshitz fit to the top RHIC energy correlation function, corresponding to the STAR experiment [8], with $r_0 = 3.23$ fm extracted from the HKM source function is presented for comparison (blue line).

The $\bar{p} - \Lambda \oplus p - \bar{\Lambda}$ correlation function (prediction for LHC)

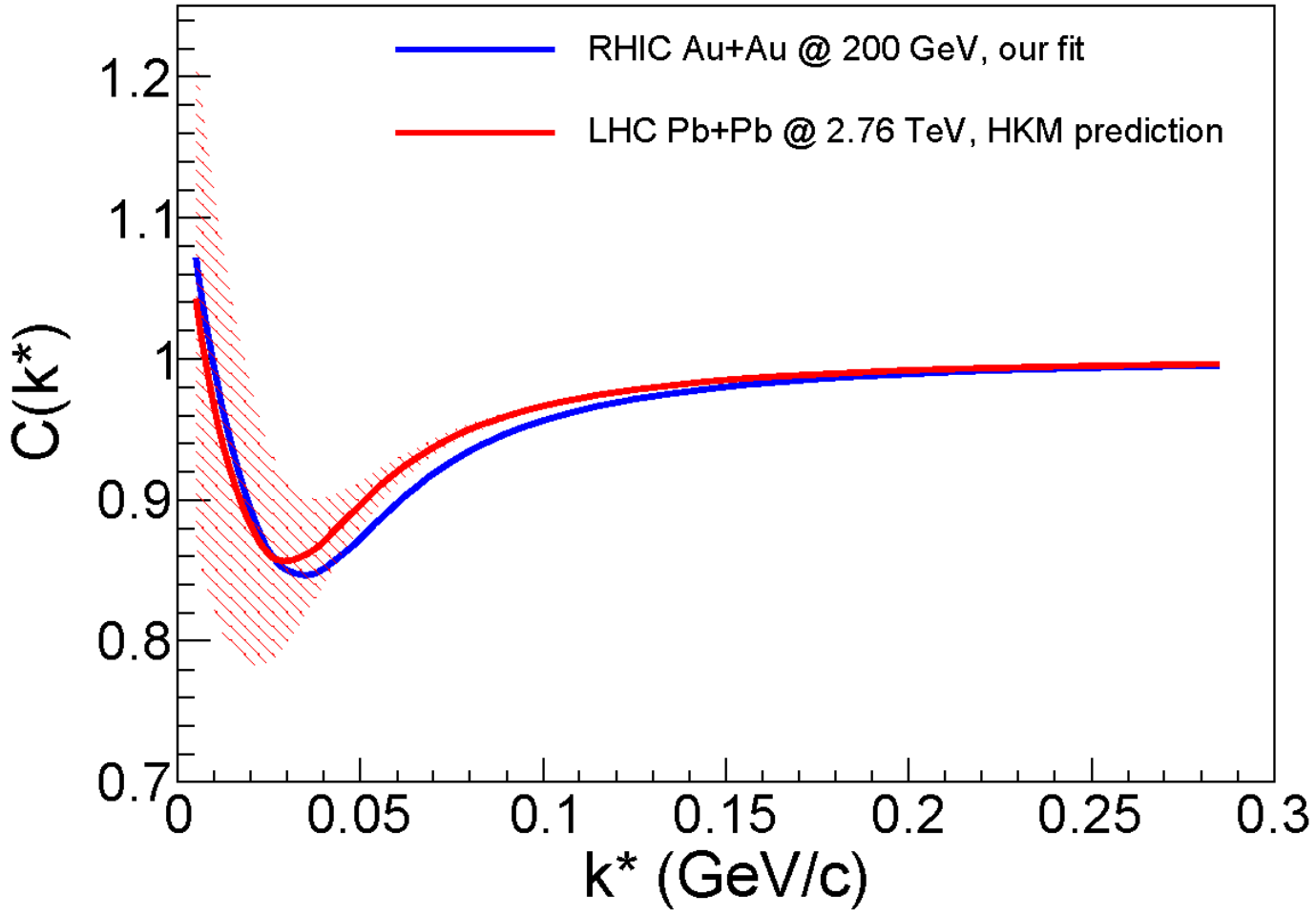

FIG. 5. The same as in previous two figures, but the correlation functions are corrected for purity and residual correlations, i. e. $C(k^*) = 1 + (C_{uncorr}(k^*) - 1)/\lambda(k^*) - \alpha(k^*)(C_{res}(k^*) - 1)/\lambda(k^*)$.

Correlation function for $p - \Xi^- \oplus \bar{p} - \Xi^+$ (prediction for the LHC)

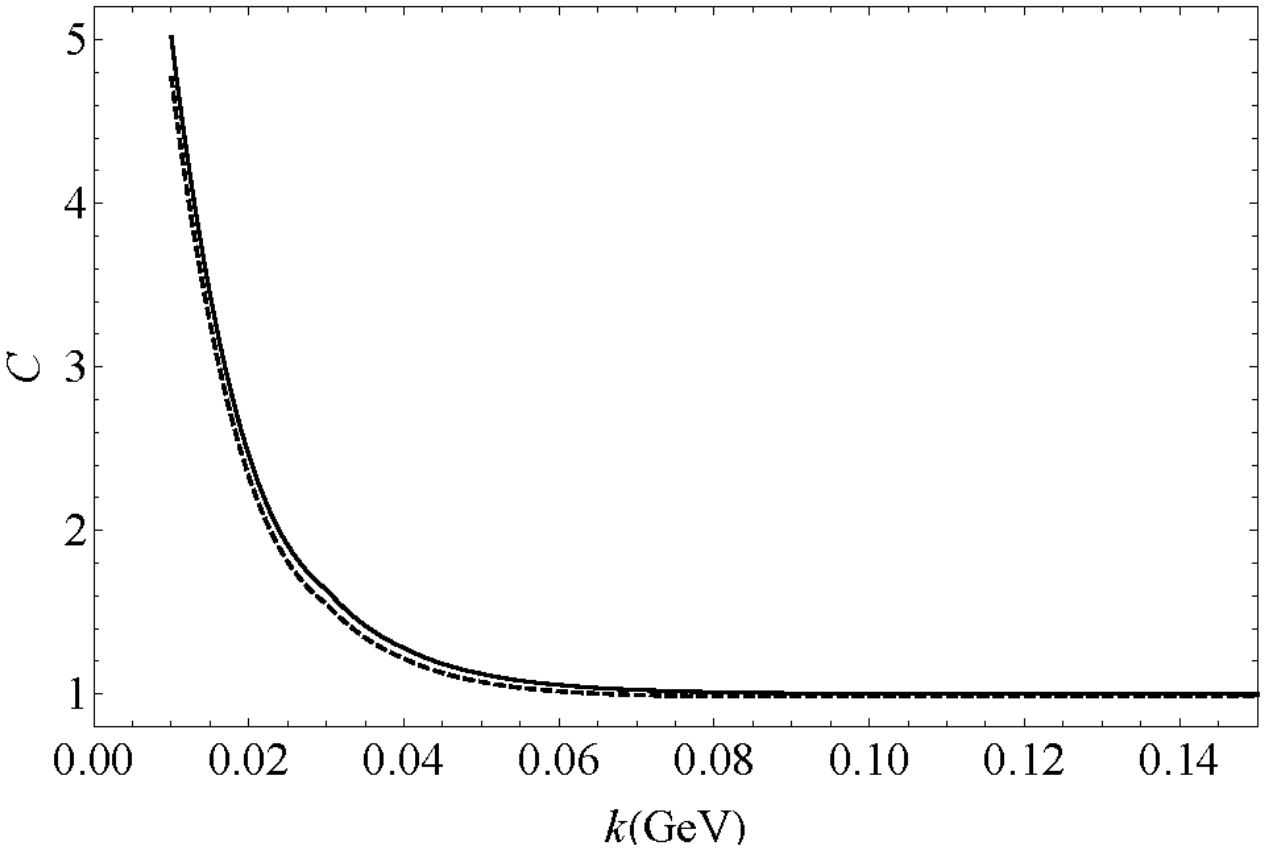

The pure (purity $\lambda = 1$) baryon-baryon correlation function between primary proton and cascade, $p\Xi^-$ obtained in iHKM simulations. The Gaussian radius in the source function distribution in iHKM is 3.1 fm. The scattering lengths for strong interactions are supposed to be the same as in $p - \Lambda$ systems. The solid line is related to utilizing the basic formula (1) for the Coulomb plus strong FSI at all distances r between the two baryons in the rest system of the pair. The dashed line corresponds to switching off all interactions at $r < 1fm$. Therefore, the realistic results, accounting for the baryon kernel in short range interaction and electromagnetic form-factors of barvons is supposed to be between these two curves.

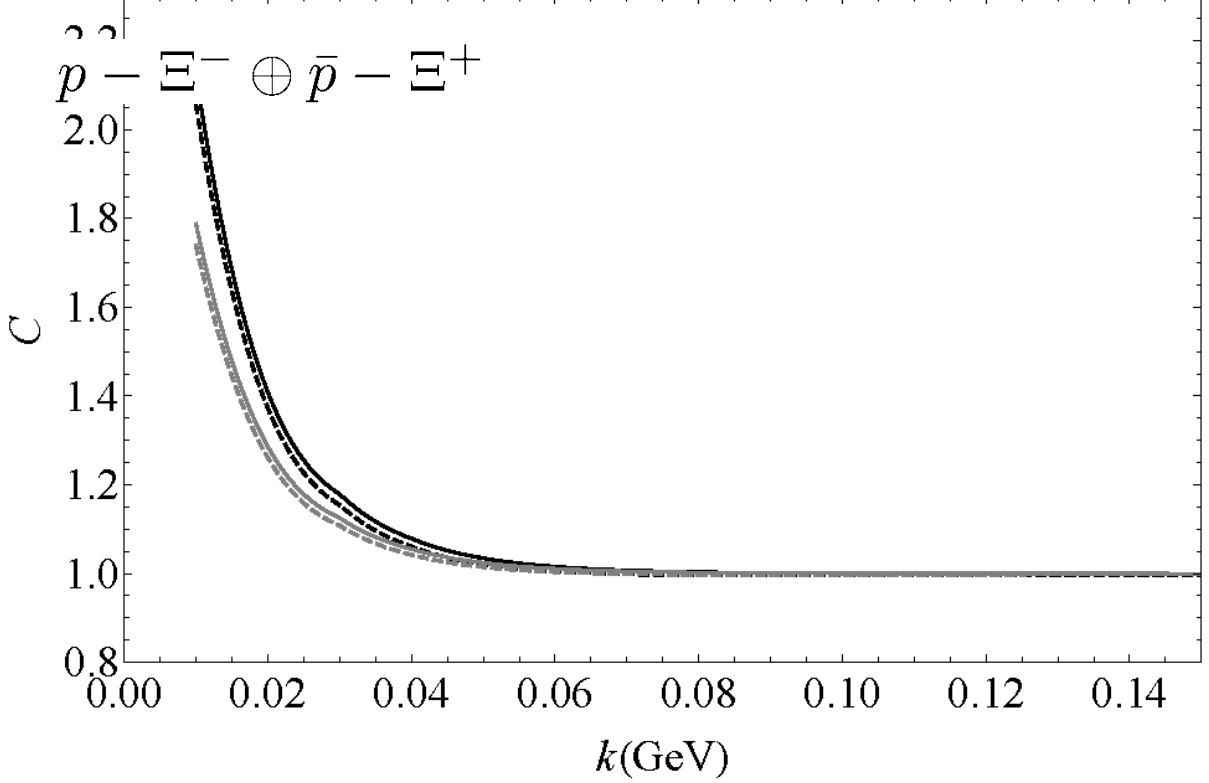

The prediction for observed baryon-baryon correlation function proton and cascade, $p\Xi^-$ obtained in iHKM simulations. The purity that is result of long-lived resonance decays is found in iHKM as $\lambda_{res} = 0.28$. The gray lines account for purity connected with particle misidentification and some other detector aspects. We put this additional factor as 0.7, so that the gray lines are corresponding to $\lambda = 0.7\lambda_{res} = 0.196$.

$\bar{p} - \bar{\Xi}^- \oplus p - \Xi^+$

Prediction for the LHC

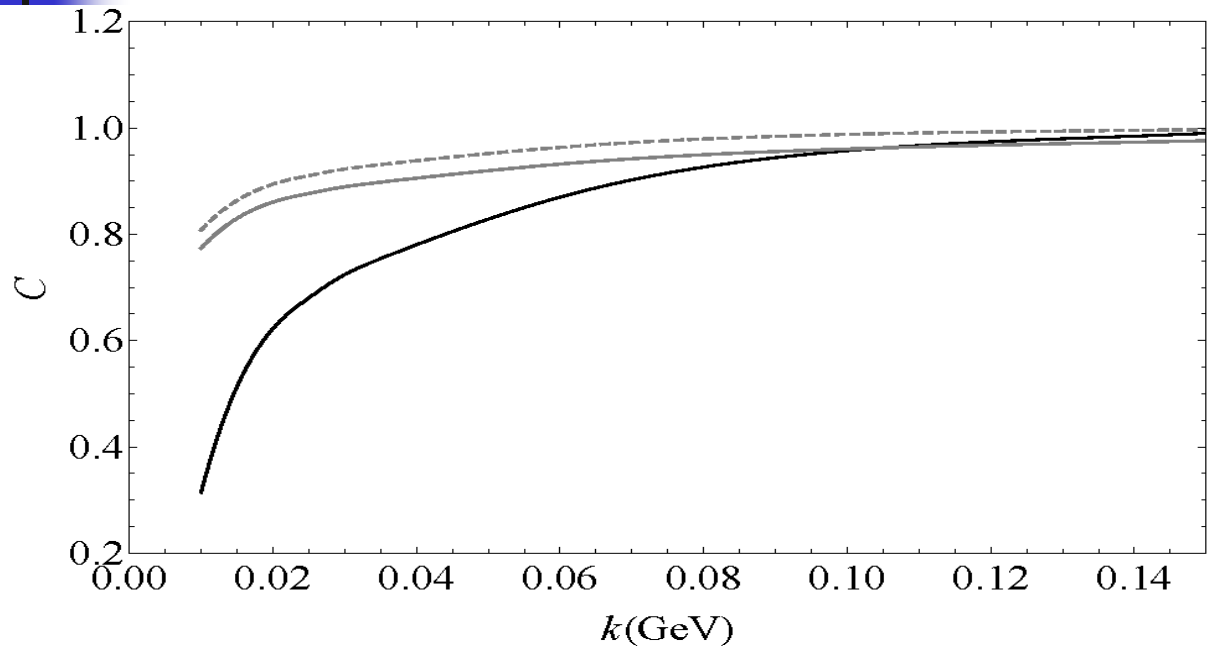

The baryon-antibaryon correlation function for primary proton and anti-cascade, $p\Xi^+$, obtained in iHKM simulations. The Gaussian radius in the source function distribution in iHKM is 3.1 fm. The scattering lengths for strong interactions are supposed to be the same as for $\overline{\Lambda}$ extracted from STAR data in Ref. [4]. The solid line is related to purity = 1 in primary baryon-antibaryon system. The gray dashed line correspond to the purity that is result of long-lived resonance decays as it found in iHKM, $\lambda_{res} = 0.28$. Solid gray line corresponds account for the residual correlations among primary parents of p or/and Ξ^+. The parameters of such a correction are taken from top RHIC energies [4] and adjust for LHC space scale by using iHKM.

Summary (iHKM)

- The integrated hydrokinetic model (iHKM) of A+A collisions is developed.
- Quite satisfactory results at different centralities are reached for multiplicities of all charged particles, pion, kaon and antiproton spectra, pion *v*_2- coefficients and interferometry radii vs transverse momentum.
- The coherent description of these observables is achieved in iHKM with the small time formation (τ_0 = 0.1 fm/c) of the maximally anisotropic initial state, with small mean relaxation time, τ_{rel} = 0.25 fm/c, and the minimal ratio of shear viscosity over entropy density $\eta/s = 1/4\pi$.
- It is observed that the isotropic initial conditions, larger relaxation time, or treatment of the pre-thermal stage just with viscous or ideal hydro-approach, leads not to dramatically worse results, if normalization of maximal initial energy densities is adjusted to reproduce multiplicity of all charged particles in each scenario.
- It can explain a rather satisfactory data description in numerous variants of hybrid models without pre-thermal stage when the initial energy densities are defined up to a common factor.

Summary (observables)

- The HKM predictions for pion and kaon radii are conformed in RHIC and LHC experiments.

- The HKM prediction for pion- kaon k_T -scaling is conformed at RHIC and LHC experiments

- The reasons for violation of m_T – scaling are intensive transverse flows and (mainly) re-scattering at the afterburner stage.

- It is found that in Pb+Pb collisions at LHC energy $\sqrt{s_{NN}} = 2.76$ GeV, $0.2 < p_T < 0.3$ GeV/c, the pion radiation is maximal at $\tau = 9.30 \pm 0.24 \pm 1.0$ fm/c and for kaons $\tau = 11.70 \pm 0.64 \pm 1.0$ fm/c.

- The latter supposed to be conditioned by K* with life-time 4-5 fm/c. It decays in hadronic medium results in suppression of the possibility of K* registration since the daughter particles are partially rescatter. The corresponding analysis is presented.

- An unexpected prediction is the m_T – scaling for Gaussian source radii for mesons and baryons pairs. Probable explanation is that source radii are defined in the pair rest frames, so it is not sensitive to transverse flow violating the scaling.

- Source functions extracted from iHKM, allows one to analyze the strong interaction in different baryon – (anti)baryon systems, including also multi-strange ones.

Thank you for your attention!